Single-cell RNA-seq reveals identity and heterogeneity of malignant osteoblast cells and TME in osteosarcoma

Yan Zhou *[1], *Dong Yang** [4], *Qing-Cheng Yang** [4], *Xiao-Bin Lv** [7], *Wen-Tao Huang** [5], *Zhenhua Zhou* [6]，*Ya-Ling Wang* [1], *Zhichang Zhang** [4], *Ting Yuan** [4], *Xiaomin Ding* [1], *Li-Na Tang* [1], *Jian-Jun Zhang* [1], *Jun-Yi Yin* [1], *Yu-Jing Huang* [1], *Wen-Xi Yu* [1], *Yong-Gang Wang* [1], *Chen-Liang Zhou* [1], *Yang Su* [1], *Ai-Na He* [1], *Yuan-Jue Sun* [1], *Zan Shen* [1], *Bin-Zhi Qian* [8], *Peizhan Chen* [#2], *Xinghua Pan* [#3], *Yang Yao* [#1], *Hai-Yan Hu* [#1]

1. Oncology Department of Shanghai Jiao Tong University Affiliated Sixth People's Hospital, Shanghai; No 600 Yishan Road Xuhui District of Shanghai City, China, 200233.
2. Clinical Research Center, Ruijin Hospital North, Shanghai Jiao Tong University School of Medicine, Shanghai, 200031
3. Department of Biochemistry and Molecular Biology, School of Basic Medical Sciences, Southern Medical University, and Guangdong Provincial Key Laboratory for Single Cell Technology and Application, Guangzhou, Guagdong Province, 510515, China.
4. Orthopaedic Department of Shanghai Jiao Tong University Affiliated Sixth People's Hospital, Shanghai; No 600 Yishan Road Xuhui District of Shanghai City, China, 200233.
5. Pathology Department of Shanghai Jiao Tong University Affiliated Sixth People's Hospital, Shanghai; No 600 Yishan Road Xuhui District of Shanghai City, China, 200233.
6. Department of Orthopaedic Oncology, Changzheng Hospital, Naval Military Medical University (The Second Military Medical University), Shanghai 200003, China
7. Central Laboratory of the First Hospital of Nanchang; No 128 Xiangshan N Road, Donghu District, Nanchang City, Jiangxi Province, China, 330008.
8. MRC Centre for Reproductive Health & Edinburgh Cancer Research UK Centre， Queen's Medical Research Institute, Edinburgh, United Kingdom, EH16 4TJ

ABSTRACT

Osteosarcoma (OS) has high heterogeneity and poor prognosis. In order to explore the molecular mechanism of OS and the tumor micro-environment (TME) on OS, we employed single-cell RNA-sequencing (scRNA-seq) on 110,745 individual cells from OS primary lesion, recurrent focal and metastatic tissues. We identified 5 main malignant subpopulations of OS cells, 3 clusters of osteoclast(OC) and 2 types of cancer-associated fibroblasts (CAFs). Further we found that the progenitor OC and, antigen presenting CAF (apCAF) were lower in lung metastatic and recurrent tumor

[1] * The first five authors contributed equally to this work.

2 # To whom correspondence should be addressed to xuri1104@163.com, panvictor@qq.com Yangyao_6@hotmail.com and pzchen@me.com. This work was supported by National Natural Science Foundation of China (No 8187215, 81503396 and 81372873) and National Key Research Project of Science & Technology Ministry(2016YFC0106204) and Shanghai Ministry Science & Technology Research Project (17411950304). Bin-Zhi Qian is supported by CRUK Career Development Fellowship C49791/A17367 and ERC Starting Grant 716379.

tissues than in primary tumor tissue. M2-like macrophages were predominant in the TME myeloid cells. Inactivation state of tumor-infiltrating T cells, mainly the CD4-/CD8- T and Treg cells, existed in lung metastatic tissues. T-cell immunoreceptor with Ig and ITIM domains (TIGIT) expressed in 11 samples. We then blocked TIGIT which significantly enhancd the cytotoxic effects of primary T cells on OS cell lines. Our report represents the first use of scRNA-seq for the transcriptomic profiling of OS cells. Thus, the findings in this study will serve as a valuable resource for deciphering the intra-tumoral heterogeneity in OS and provide potential therapeutic strategies for OS in clinic.

Introduction

Osteosarcoma (OS) is a highly aggressive malignant bone tumor frequently occurring in children and adolescents[1-3]. The incidence of OS is about 4.8 per million per year. Traditionally, the standard treatment protocol for OS consists of extensive surgical resection, chemotherapy, and radiation. Researchers have been screening the effective target drugs on OS for decades. In recent years, the vascular endothelial growth factor receptor- tyrosine kinase inhibitors (VEGFR-TKIs) have appeared outstanding due to their effectiveness. However, as stated by the Surveillance, Epidemiology, and End Results (SEER) Program, the five-year overall survival rate for patients with bone sarcoma is 66.2% (2009 to 2015)[4]. According to the published data, the relapse and/or metastasis rate of OS remains to be higher than 30%. For these patients, the five-years overall survival rate was even worse, being about 10–30% [5]. As such, there is an urgent need to identify the molecular mechanism and novel therapeutics that may improve management of OS.

Immune checkpoint inhibitors have led to a breakthrough in immunotherapy for a variety of solid tumors [6,7]. However programmed cell death 1 (PD-1) inhibition has limited effect in OS[8,9]. Davoli revealed that highly aneuploid tumors showed reduced expression of markers of cytotoxic infiltrating immune cells, especially CD8+ T cells, and increased expression of cell proliferation markers. Immune evasion markers correlated mainly with arm- and chromosome-level somatic copy number alterations (SCNAs), consistent with a mechanism related to general gene dosage imbalance rather than the action of specific genes. In this regard, OS is the typical one [10]. Previous reports show that OS is abundant in widespread and recurrent somatic chromosomal lesions, including structural variations (SVs) and copy number alterations (CNAs); however, few recurrent point mutations in protein-encoding genes have been identified in OS[11-15].Low expression of immune-associated genes is

another significant phenotype for OS[16]. How to convert the immunosuppressive microenvironment into the one that favors the induction of antitumor immunity is indispensable for effective cancer immunotherapy.

Here, we employed single cell transcriptome approach to dissect the heterogeneity of OS cells. We analyzed the transcriptomic profiles of a total of 110745 cells from 7 primary tumors, 2 lung metastatic and 2 recurrent OS tissues. We first divided the OS cells into 5 sub-clusters and osteoclast into 3 subtypes. The profiles of OS, OC and immune-system cells were analyzed. We found that the TME of the recurrent and lung metastatic OS exhibited more significant suppressivity than primary tumor tissue. Thus, the results in this study improve the understanding of the immune-suppressivity observed in advanced OS including distant metastasis and recurrence, and are potentially valuable in novel treatment strategy for OS.

Of importance, we are the first to uncover that Treg cells in OS expressed TIGIT. TIGIT is a coinhibitory receptor expressed on effector T cells, natural killer (NK) cells, T regulatory cells (Treg) and T follicular helper (TFH) cells. It has gained attention as a potential therapeutic target in wide variety of tumors[17-19]. The antibodies of TIGIT, named BGB-A1217, had registered and recruited on August 2019. Here we explored the preclinical significance of blocking of TIGIT.

Method

Patients

The eleven patients for scRNA-seq analysis enrolled in this study were hospitalized during the period of October 2017 to April 2019 in Shanghai Sixth People's Hospital. The study was approved by Shanghai Sixth People's Hospital Ethics Committee. Each patient was provided a written signed consent. All patients were diagnosed according to the National Comprehensive Cancer Network (NCCN) Clinical Practice Guidelines in Oncology with the terms of Bone Cancer (Version 2.2019). Among 11 patients for scRNA-seq, 7 were derived from the primary sites of patients who received traditional first line combination chemotherapy for OS, including Adriamycin(ADM), cisplatin(DDP), methotrexate(MTX) and Ifosfamide(IFO) and surgical therapy. 2 lung metastatic patients and 2 recurrent patients all received the gemcitabine combined with Docetaxel(GT) chemotherapy treatment. The BC17, one of the lung metastasis patients, had enrolled in clinical trial NCT03676985 and undergone the anti-PD-L1 treatment for 6 times. For this clinical trial, all enrolled patients had finished the neoadjuvant chemotherapy, operation and adjuvant chemotherapy. They would accept

anti-PDL-1 for one year until the disease progresses. Detailed information of the 11 patients was provided in Table 1 respectively. Tow patient agreed to donate blood for us to explore the effect of anti-TIGIT.

Sample preparation and cell purification for scRNA-seq

The fresh tumor tissue was stored in the GEXSCOPETM Tissue Preservation Solution (Singleron) and transported to the Singleron lab on ice as soon as possible. The specimens were washed with Hanks Balanced Salt Solution (HBSS) for 3 times and minced into 1–2 mm pieces. Then the tissue pieces were digested with 2 ml GEXSCOPETM Tissue Dissociation Solution (Singleron) at 37℃ for 15 min in 15 ml centrifuge tube with sustained agitation. After digestion, the samples were filtered through 40-μm sterile strainers and subsequently centrifuged at 1,000 rpm for 5 minutes. Thereafter, the supernatants were discarded, and the cell pellets were suspended in 1 ml PBS (HyClone). To remove the red blood cells, 2 mL GEXSCOPETM red blood cell lysis bu□er (Singleron) was added at 25°C for 10 minutes. The solution was then centrifuged at 500 × g for 5 min and suspended in PBS. The sample was stained with trypan blue (Sigma) and evaluated microscopically.

10x library preparation and sequencing

Single-cell suspensions were converted to barcoded scRNA-seq libraries by using the Chromium Single Cell 3'Library, Gel Bead & Multiplex Kit (10x Genomics, V3), and following the manufacturer's instructions. Briefly, cells were partitioned into Gel Beads in Emulsion in the ChromiumTM Controller instrument where cell lysis and barcoded reverse transcription of RNA occurred. Libraries were prepared using 10x Genomics Library Kits and sequenced on Illumina HiSeq X with 150 bp paired end reads.

Raw reads were processed to generate gene expression profiles using an internal pipeline. Briefly, after filtering read one without poly T tails, cell barcode and UMI was extracted. Adapters and poly A tails were trimmed (fastp V1) before aligning read two to GRCh38 with ensemble version 92 gene annotation (fastp 2.5.3a and featureCounts 1.6.2). Reads with the same cell barcode, UMI and gene were grouped together to calculate the number of UMIs per gene per cell. The UMI count tables of each cellular barcode were used for further analysis. Cell type identification and clustering analysis using Seurat program. The Seurat program

(http://satijalab.org/seurat/, R package, v.3.0.1) was applied for analysis of RNA-Sequencing data.

Cell-type identification and subgroup categorization by the t-SNE method.

The individual Seurat objects were integrated with the SCTransformation algorithm provided by the Seurat package. The top 3,000 Highly variable genes across the cells were chosen to perform the Principal Component Analysis(PCA) analysis. Top 50 significant PCAs were applied for the graph–based clustering based on the t-SNE method to identify the main cell groups for all samples. In the subgroup cell identification, the top 10 PCAs were applied for the graph based clustering. The cells in each integrated subcluster were selected to run the SCTransformation analysis with the cells being categorized with the top ranked, differentially expressed genes and the well-known cellular biomarkers. The osteoclast cell biomarkers were defined as the cathepsin K5(CTSK5) and tartrate-resistant acid phosphatase(TRAP/ACP5); cadherin11(CDH11), Integrin Binding Sialoprotein (IBSP) for osteoblast cells; lumican(LUM), decorin(DCN), collagen, type I, alpha 1(COL1A1) for fibroblast; CD74, CD68 for monocytes; CD2, natural killer cell granule protein 7(NKG7) and CD3D for T and NK cells.

Differential expressed genes(DEG) identification and Gene Ontology(GO) enrichment analysis

The cluster subgroup specific biomarkers were identified with the FindAllmarkers functions implemented in the Seurat package based on the normalized gene expression data. The genes with the adjusted P-values < 0.05 between the clusters were defined as DEGs and were selected for the GO enrichment analysis using the ClusterProfiler package of R.

CNV estimation in the OS tumor

Initial CNVs for each region were estimated by inferCNV R package. The CNVs of total cell types were calculated by expression level from single-cell sequencing data for each cell with –cutoff 0.1 and –noise_filter 0.2. For each sample, gene expression of cells was re-standardized and values were limited as −1 to 1.

Construction of single cell trajectories of OS cells

To identify genes that were involved in the progression of OS cells, the Monocle2 package (v2.8.0) was used to analyze single cell trajectories from primary tumor to the lung metastasis or recurrence. We used top 100 differentially expressed genes across the cell types identified by the Monocle 2 to sort the cells in pseudo-time order. The

gene expression files in the primary cells were defined as the root_stage and the DDRTree was applied to reduce the dimensions and visualize the plot_cell_trajectory functions implemented in the monocle2. Differentially expressed genes over the Pseudo-time from primary tumor to lung metastasis or recurrent were calculated by the "differentialGeneTest" function in Monocle2 (q value < 10^{-20}). The genes were categorized into 6 subgroups and the GO function enrichment analysis was performed for the genes in each cluster with the ClusterProfile package of R.

Immunohistochemistry(IHC) staining and immunofluorescence(IF) staining

Tissue sectioning and IHC staining of formalin fixed paraffin-embedded (FFPE) OS specimens were performed following the general methods. All sections were deparaffinized, rehydrated, and washed and endogenous peroxidase was blocked using3% H_2O_2 for 10 min, the slides were incubated with primary antibodies followed by HRP-linked secondary antibodies and diaminobenzi- dine (DAB; ZhongShan Golden bridge biotechnology Co LTD, Cat No. ZLI-9018) staining. Counterstaining was done with hematoxylin. Slides were dehydrated with sequential ethanol washes for 1 min each starting with 75%, followed by 80% and finishing with a 100% ethanol wash. Two physicians blinded for clinical/tumor-characteristics independently assessed IHC-staining for TIGIT, CD3, CD4, CD8, CD74 and CTSK.

For IF staining, the process was same to above until inncubating with primary antibodies overnight at 4°C. Fluorescence-labeling secondary antibodies including donkey anti-rabbit Alexa Fluor488 (Molecular Probes, catalog A21202, 1:1000) and goat anti-mouse Alexa Fluor 514nm (Molecular Probes, catalog A31555, 1:1000) were incubated for 1 hour at room temperature after washing. Nuclei were counterstained with DAPI (MilliporeSigma, D9542). Sections were mounted using fluorescence mounting medium (Dako, S3023).

Cytotoxicity assays by CytoTox 96® Non-Radioactive Cytotoxicity Assay

PBMCs were collected from BC3 and BC16 by density centrifugation using Lymphocyte Separation Medium (MP Biomedicals). Then CD3+ T cells were isolated using the MACS positive selection technology (Miltenyi Biotec) according to the manufacturer's protocol. For T-cell activation assays, CD3+ cells were seeded in 24-well plates and stimulated with IFN-y(1000 U/mL; Peprotech), IL-2 (600 U/mL, Peprotech) and anti-CD3 antibody (5 ng/mL, clone OKT3; Biolegend) for 3 days then blocked TIGIT with TIGIT antibodies(50 μg/ml, clone #A15153G, Biolegend) for

24h. 143B and U2OS cells were seed in 96-well plates overnight, then added CD3+ T cell at effector-to-target (E:T) ratios of 4:1 and 8:1. Co-culture system were incubated for 8 h. The supernatant was harvested and was subjected to analysis by the CytoTox 96® Non-Radioactive Cytotoxicity Assay. The killing effect of T cells against target cells was assessed with the following equation: Cytotoxicity = (Experimental – Effector Spontaneous – Target Spontaneous)/(Target Maximum–Target Spontaneous) × 100%. All experiments were performed at least three times.

Statistical analysis

Statistical analysis was performed using statistics package for social science 21.0 (SPSS 21.0; SPSS Inc, Chicago, IL). All the data were expressed as mean±SD. The significance was determined by the t test. $p<0.05$ was considered statistically significant.

Results

Single-cell analysis uncovers the complexity of OS tumor

To explore the cellular compositions in OS, we performed scRNA-seq analysis of 7 primary OS tumors, plus 2 recurrent OS tumors, and 2 samples from pulmonary metastasis (Table 1). After initial quality control, we acquired single-cell transcriptomes in a total of 110,745 cells, including 72,004 cells from *in situ* samples, 19,439 cells from lung metastasis samples, and 19,302 cells from recurrence samples. We first applied principle component analysis on variably expressed genes across all cells and identified six main cellular clusters including OS (osteoblast cell, 47,598), osteoclast cell (9,180), fibroblast (26,772), myeloid cell (18,158), endothelial (3,621) and T/NK cell (5,416) based on the t-distributed stochastic neighbor embedding (t-SNE) analyses in two dimensions (Fig. 1A). The t-SNE results for individual patients were shown in Supplementary Fig. S1. We performed the differential expression analysis to identify the cellular cluster-specific genes and defined the cellular cluster together with the well-known cellular biomarkers. The dot-plot and violin-plot showed the well-known cell type-specific markers embedded in cells from distinct clusters (Fig. 1B and C). The heatmap gathered the well-known cell type markers to distinguish each cell cluster, such as CTSK, ACP5 for osteoclast, CDH11 and BSP for malignant osteoblast, which we defined here as OS cell.

Intra-tumoral heterogeneity in malignant OS cells

With the t-SNE analysis of osteoblast OS cells, we identified 5 distinct subgroups, named as metabolic, proliferating, extracellular matrix remodeling, ossification and cellular differentiation cells, respectively (Fig. 2A). Based on the GO analysis, cluster 1 was enriched in genes related to structural constituent of ribosome, glycolysis and active lipid metabolism and therefor termed as metabolic OS cells. Cluster 2 was enriched in genes related to cell cycle and proliferating with relatively higher expression of Ki67 and TOP2A and termed as proliferating OS cells. Cluster 3 was enriched with genes related to extracellular matrix modeling and therefor defined as ECM modeling OS cells. Genes in cluster 4 had a high level of genes involved in sulfur compound binding, heparin binding and glycosaminoglycan binding pathway, suggesting it was associated with ossification and therefor defined as ossification. Cells in cluster 5 were specific in cell differentiation processes including histone acetyltransferase binding, RNA polymerase II transcription factor binding and DNA−binding transcription activator activity. Many transcription factors, such as JUN, MYC, SOX9, etc, were over-expressed, suggesting that they may be pluripotent (Fig. 2B), and the cells were defined as cellular differential OS cells. The KEGG analysis showed that the genes of TP53 pathway were markedly disordered in subgroup 5 (Fig. S2A). The heatmap displayed the key genes characterizing our classification (Fig. S2 B).

To address the origin differentiation, development and stemness of OS, we performed the trajectory analysis of OS cells(Fig. 2D). Firstly we evaluated the genes that expressed along with the pseudo-time in primary OS cells. It is uncertain which cell type is responsible for OS initiation. Our data imply that in the primary OS tissue, the highly proliferating OS cells would transit to the differentiation cells with transcription factor including, over-expression and then transform to special potential cells including hypermetabolism, bone matrix remodeling and ossification. We further analyzed the gene patterns along with the cellular trajectories, and the genes were subclustered into 4 groups. The GO analysis suggested that the genes related to mitotic nuclear division were down-regulated along with the trajectory while genes related to regulation of ossification and bone morphogenesis were increased along with the trajectory.

Secondly, we performed the cellular trajectories from primary to lung metastasis. In the lung metastasis, the genes were categorized into 6 clusters, with the genes related to cellular matrix being significantly down-regulated, while the genes

related to mitotic nuclear division, organelle fission, RNA catabolic process, nuclear transcribed mRNA catabolic process nonsense mediated decay and cotranslational protein targeting to memberane *etc.* were significantly increased. Furthermore, ten transcriptional factors, including (SRY-like HMG box) SOX2, TP73, and homeobox gene family D11 (HOXD11) *etc.,* were significantly increased in the lung metastasized cells, suggesting that they play important roles in lung metastasis of OS cells.

Thirdly, we explored the cellular trajectories from primary to recurrent OS cells. The genes in response to IFNγ were reduced while genes related to the connective tissue were significantly increased. Thirty-one transcriptional factors, including MYC, FOS, ORF of iroquois homeobox 1 (IRX5) and JUNB *etc.,* were significantly increased in the local tumor recurrence, suggesting that they play vital roles in the diseases recurrence.

We also calculated large-scale chromosomal CNV in each subject based on averaged expression patterns across intervals of the genome (Fig. S3). We found that, while the genomic region of 8q was frequently increased in the OS cells, 6p region was frequently down-regulated, which were in consistent with previous studies performed with the CGH methods[20].

From antigen presenting to bone resorption during the OC maturation

The bone or bone-like microenvironment/niches provide growth and survival signals essential for OS initiation and progression. OC is an important type of cells to maintain the balance of bone formation. Previous studies suggested that OC cells express immune regulators, uptake soluble antigens and secrete cytokine to activate both CD4+ and CD8+ T cells in an MHC-restricted fashion[21]. Mature osteoclast (OC) is a type of poly-nuclear cell involved in the bone resorbing. We hypothesize whether the function of OCs dynamic change with development. Here we divided the OC cells into 3 main subgroups based on the integration data, including progenitor OC, immature OC and mature OC cells(Figure 3A) The progenitor OC cells showed relatively higher CD74 and the topoisomerase IIα (TOP2A), while the mature OC cells displayed higher expression of CTSK and ACP5 (Fig. 3B). The cellular trajectory analysis is consistent with our hypothesis that the cells with higher CD74 expression level were ranked at the origin of the pseudo-time linkage while the expression of CTSK and ACP5 were increased along with the pseudo-time(Fig. 3C).

The primary function of CD74 is regulation of T-cell and B-cell developments, dendritic cell (DC) motility, macrophage inflammation, and thymic selection[22]. In addition CD74 can act as a receptor for macrophage migration inhibitory factor (MIF). It was found that MIF inhibited osteoclast formation and CD74 knockout (KO) mice had decreased bone mass[23]. We detected the CD74 and CTSK co-expression in OCs by IHC method on serial section. We found the cells with CD74 extreme positive were small and mononuclear with weakly positive of CTSK. The CD74 level in multinuclear OCs presenting light brown was markedly lower than in mononuclear OCs(Fig. 3D). The IF results were equal to IHC(Fig. S5). This result also indicated that the antigen presentation function of OC fade away with its development.

Furthermore, we analyzed the gene change in 25 GO biological process categories. The genes related to antigen processing and presentation via MHC class IB, aminoglycan catabolic process, collagen fibril organization *etc*, showed a significant increase along with the differentiation of OC cells, while the genes related to sequestering of metal ion, bone mineralization, extra cellular structure organization *etc*, were down-regulated with the differentiation (Fig. 3E, Fig. 3F). For our opinion, along with the differentiation of OC, the antigen presenting function was diminishing, while the bone resorption function became stronger and stronger. The deficiency of progenitor OC in metastasis and recurrent OS tissue may contribute to the immunosuppressed state.

Distincted capCAFs in OS

CAFs modulate tumor stiffness and facilitate cancer progression. Based on the reported CAF biomarkers including land use Lumican(LUM), collagen type I alpha 1 chain(COL1A1) and decorin(DCN), a total of 18,158 fibroblast cells were identified. These fibroblast cells were categorized into two distinct subclusters (Fig. 4A), including myofibroblastic CAFs (myCAFs) with periglandular FAP+ αSMA^{high} and apCAFs with high level of MHC class II family members [24]. Compared to the myCAFs, the apCAFs showed relative higher expression level of CD74 and the MHC II molecules while the expression level of DCN and LUM was relatively lower (Fig. 4B). We then generated the heatmap according to cluster-specific marker genes by performing differential gene expression analysis to define the identity of each cell cluster (Fig. 4C). It's worth noting the apCAFs were frequently identified in the primary tissue (1335/4587), but rarely noted in the metastasis (226/5000) and the recurrent tumors (452/5217), implying the antigen presenting was more active in

primary OS tissue.

Functional analysis of the myeloid cells in OS

Tumor□infiltrating myeloid cells are the most abundant monocyte population within tumors and known for their functional and molecular plasticity. In this paper, we identified 7 subgroups of the myeloid cells, including the M1-like macrophage, M2-like macrophage, IFN activated macrophage, CD14+ monocyte, DC, proliferating myeloid cells and neutrophil cells (Fig. 5A). Each subgroup of the myeloid cells had distinctive biomarkers, which were shown in violin-plot (Fig. 5 B).

Tumor-associated macrophages (TAMs) are the major immune component of myeloid cells in OS. The majority of the TAMs have relatively higher expression level of CD163 and mannose scavenger receptor(MRC1)/CD206, suggesting that these cells were M2-polorized TAMs in OS (Fig. 5 C). The TAMs were clustered into 3 subgroups. The first group was the M1-like TAMs expressing a relatively higher level of pro-inflammatory markers including C-C motif chemokine ligand 2(CCL2), CCL3, CCL4, CXC motif chemokine ligand 2(CXCL2) and CXCL3. The main ingredient was M2-like TAMs with relatively higher expression of inflammatory biomarkers including IL-10. We also found the IFN activated macrophage, which was characterized with higher expression levels of IFN-induced proteins with tetratricopeptide repeat 1(IFIT1), IFIT2 and IFIT3, suggesting that the activation of IFN signaling pathway may contribute to the tumor suppressive microenvironment (Fig. 5D). Our data imply OS is abundant in M2-like immunosuppressive TAMs.

Contribution of the immune-suppressive tumor-infiltrating Lymphocyte(TIL) cells to OS

The presence and content of TILs is considered to be closely related with response to the immunotherapy[25]. Here we characterized the subpopulations of TIL using transcriptomic patterns. According to the analysis, the major groups of the lymphoid cells included CD4-/CD8- T cells, CD8+T cells, NK cells, T-reg cells, mast cells and plasma cells (Fig.6A). The lymphoid cells were the majority in the primary tumor and the lung metastatic tumor. In contrast, they were rarely noted in the recurrence tumor samples. Most of the T cells in the primary OS tumor were CD4-/CD8- T and Treg cells. In the lung metastasis, about 311 out of the 1969 T cells were T-reg cells. Meanwhile, the cellular distribution of NK cells and the CD8+T cells were significantly reduced in the lung metastatic tumors. Using the IHC method (Fig. 6B),

we validated the cellular composition of the lymphoid cells, and found that cytotoxic CD8+T cells barely existed in the recurrent and lung metastatic tumors. Our results suggested the cytotoxity of T cells is loss-of-function in the OS tumor, especially in recurrent and metastatic tissue.

We performed the dot-plot analysis to display the level of marker genes in all kinds of cells (Fig. 6C). The GZMB expression level was reduced, suggesting that CD8+T cells in the OS cells had lower cytotoxic activities. The cellular composition of the T-reg cells was significantly increased, and the T-reg cells expressed relatively higher levels of cytotoxic T-lymphocyte-associated protein 4(CTLA-4) and TIGIT, which are negative regulator for the cytotoxicity of the CD8+T cells (Fig. 6D).

Blocking TIGIT improved the cytotoxicity of Cytokine induced T cells (CITs) to OS cells

TIGIT is expressed normally by activated T cells, regulatory T cells (Treg), and natural killer (NK) cells, which is recently emerging as novel candidate in immunotherapy. As mentioned above, we show for the first time that the TIGIT over-expressed on TILs of OS patients by scRNA-seq. It was verified by IHC method(Fig. 7A). In order to demonstrate the therapeutic potential of TIGIT in OS, We isolated the CD3+ T cell and blocked the inhibitory activity of TIGIT. The immune cell-mediated lysis of CITs on OS cells was measurably enhanced by the addition of blocking TIGIT antibodies in co-culture system($p<0.05$, Fig. 7B).

Discussion

WES/WGS data or transcriptomic results had described OS is a highly inter-heterogeneous tumor[26]. However, they are only reflecting the average of expression levels across the tumor cells. As such, these studies could not identify cell types, nor predict developmental trajectories, clarify taxonomic composition and metabolic capacities of TME. In the present study, we applied scRNA-seq strategy to profile malignant cells and TME components from primary, recurrent and lung metastatic OS tissues. To our knowledge, this paper is the first study which performed scRNA-seq to identify the intra-heterogeneous of OS. Thus, how to identify the OS cells is most important. Han et al proposed that Ctsk+ cells serve as a physiologic and pathological precursor in osteogenic tumor[27-29], and we chose it as one of the major indicators. Meanwhile, bone sialoprotein (BSP) is thought to function in the initial mineralization of bone and selectively expresses by differentiated

402 osteoblast[30]. Here, the OS cells were characterized using CDH11，BSP, LUM, DCN
403 and COL1A1 as markers.

404 In the subgroup analysis, we put emphasis on the subtype 5 enriching in multiple
405 singling pathways related to cancer development and other transcriptional
406 misregulation signaling pathways. Meanwhile, the genes related to p53 downstream
407 signaling pathways were significantly enriched in the subcluster. As we know, TP53
408 and Rb1 exhibited the most frequent mutations in OS, which may be the initiating
409 factors for OS tumorigenesis[30]. The OS cells with TP53 mutation exhibit a high
410 chromosomic instability and lead to secondary genetic aberrations in new cancer cell
411 clones that emerged from the initial monoclone [31]. A large number of animal
412 models are developed for osteosarcoma, including P53 knock out mouse model [32].
413 Based on our cellular trajectory analysis, the precursor of OS is highly proliferative. It
414 is widely accepted that the stem cell could renew but being at G0 stage with
415 proliferative inactivity. We were unable to capture the stem cells, probably due to
416 their extremely low number. In our opinion, the differentiation subtype may be the
417 secondary genetic aberrations, which would then transform to special metabolism,
418 bone matrix remodeling and ossification subtypes. We hypothesize that the
419 components in our paper behave just like myeloblast, promyelocyte and so on, thus
420 presenting the hematopoietic cell differentiation and development processes. Of
421 course more research is necessary to further explore this hyopthesis.

422 Emerging immune checkpoint inhibitors have been the landmark treatments for
423 their clinical success in a variety of human cancers. However, the therapeutic
424 efficacies by immune checkpoint inhibitors were variable for the treatment of OS
425 patients[33,34]. Gomez-Brouchet et al. reported that PD1/PDL-1 staining was
426 negative in >80% of OS cases (n=124) [35]. Alves showed that OSJ displayed a
427 microenvironment with low tumor infiltrating lymphocytes (TILs), and few cells
428 exhibited immunotherapeutic targets CTLA-4 and PD-1[36]. Palmerini examined the
429 TAMs by primary OS tissue microarray to evaluate the status of the
430 immune-infiltrates in OS. Most cases presented TILs, which contained CD3+ (90%)
431 and CD8+ (86%). Meanwhile, PD-L1 expression was found in 14% patients in
432 immune-cells and 0% in tumoral cells [37]. Our results were consistent with theirs:
433 low cytotoxic TILs were usually in OS and the level of PD-L1 was so low that it
434 could not be detected in OS tissue. On the contrary, some previous studies on OS

435 samples reported a higher rate of positive expression of PD-L1 (IC), ranging from 25%
436 to 74% [38,39]. We reason that these variant conclusions could be ascribed to
437 insufficient statistical samples and different agents. In order to comprehensively
438 predict the validity of ICIs, more indicators are required.

439 Wang reported that metastatic OS tumors showed improved immunogenicity.
440 But most of TILs in lung metastasis were the naïve T cells or T-regs with lower
441 anti-cancer activities[40]. These results thus appeared inconsistent. In our research,
442 we found that the immunosuppression of lung metastasis tissue was more significant
443 with the higher percentage of T-reg cells. In fact, it is controversial whether metastatic
444 OS tumor was immunogenic. Our view is that significant immunophenotypic
445 disturbances were found in recurrent and metastatic tissues, with immune-cells being
446 rarely noted in recurrence OS tissue. Our data suggested that the OS immune
447 environment became "cool" in the recurrent OS tumor. Thus, we initiated the clinical
448 trial NCT03676985 using anti-PD-L1 as maintenance after adjuvant chemotherapy.

449 Another key finding of our paper is that the T-reg cells had a relatively higher
450 TIGIT expression level in OS tumor. TIGIT and its ligand poliovirus receptor (PVR)
451 have been emerging as novel promising targets in immunotherapy for many tumors
452 such as breast cancer, lung cancer, hepatocellular carcinoma etc[41-43]. Tian reported
453 that blockade of TIGIT prevented NK cell exhaustion and elicited potent anti-tumor
454 immunity[44]. In the current study, we observed that the T-reg cells had relatively
455 higher TIGIT expression level in OS tumor and blockade of TIGIT improved the
456 cytotoxicity of CIT, which suggested that OS patients may benefit from
457 individualized immunotherapy according to the genetic results.

458 TAMs are known to participate in tumor initiation, progression and metastasis.
459 We found that the majority of the TAMs have relatively higher CD206 and MRC1
460 expression, suggesting that TAMs were M2-type with anti-inflammatory activities in
461 OS tumor. Interestingly, we also observed a subgroup of TAMs with relatively higher
462 expression level of inflammatory factors including CCL3, CCL4, CXCL8 etc.,
463 suggesting that the inflammatory activities may be involved in the tumorigenesis and
464 progression of OS tumor. Our scRNA-seq analysis displayed the dynamic
465 development of TAMs, which was consistent with previous studies reported by
466 Dumars et al. that M2-macrophages were dominated in OS tissue and that
467 macrophage dyspolarization was associated with metastatic process in OS patients
468 [45]. In this regard, our data seems to offer some hints as to why the mifamurtide, a

fully synthetic lipophilic derivative of the muramyl dipeptide (MDP) encapsulated into liposomes, was effective when used together with chemotherapy for localized OS; hence, the addition of mifamurtide was preferred in non-metastatic OS patients, whereas there was no significant difference in overall survival rates between the combined use of mifamurtide with chemotherapy and chemotherapy alone in metastatic OS [46].

In recent years, CAFs have attracted attention due to their role in mediating collagen crosslinking with malignant cells by disintegrating metalloproteinases (ADAMs) and secreting multiple cytokines, chemokines and growth factors[47]. Meanwhile, CAFs assist cancer cells in evading immune surveillance through inhibiting the activity of immune-effector cells and recruiting immune-suppressive cells, thus supporting cancer tumorigenesis and metastasis[48]. However, the role of the CAFs in driving tumorigenesis of OS remains to be further elucidated. As mentioned above，Elyada et al[49] described a new population of CAFs that displayed relatively higher expression of MHC class II and CD74 without the expression of classic costimulatory molecules, and they named it "antigen-presenting CAFs". In our study, we also isolated two subtypes of CAFs, apCAFs and the traditional myCAFs. Previous studies suggested that apCAFs could activate CD4+ T cells and act as the immune-modulator [50]. We found the ratio of apCAF/myCAF in primary tumor tissue was dramatically higher than that in pulmonary metastatic and recurrent tumor tissues, suggestive of the difference of the TME of OS in the primary *versus* the metastatic tumor. Nonetheless, more studies are warranted to address the origin of the apCAFs and their roles in the OS progression and development.

In summary, using the scRNA-seq method, our study uncovers the intra-heterogeneity of both malignant OS cells and the TME. Distinct subgroups of OS cells were documented and the cellular lineage in lung metastasis of OS were determined. Furthermore, the main immune cell types in the TME were profiled. Together, our findings in the present study may provide novel therapeutic targets and methods for the treatment of OS patients.

ACKNOWLEDGMENTS

We thank all the patients who contributed to this study. We also thanks the Hengrui pharmaceutical co. LTD due to providing the antibodys of TIGIT and CTSK for free.

Reference

1) Pingping B, Yuhong Z, Weiqi L, Chunxiao W, Chunfang W, Yuanjue S, Chenping Z, Jianru X, Jiade L, Lin K, Zhengdong C, Weibin Z, Chen F, Yang Y. Incidence and Mortality of Sarcomas in Shanghai, China, During 2002-2014. Front Oncol. 2019 Jul 17;9:662.

2) Lancia C, Anninga JK, Sydes MR, Spitoni C, Whelan J, Hogendoorn PCW, Gelderblom H, Fiocco M. A novel method to address the association between received dose intensity and survival outcome: benefits of approaching treatment intensification at a more individualised level in a trial of the European Osteosarcoma Intergroup. Cancer Chemother Pharmacol. 2019 May;83(5):951-962.

3) Siegel RL, Miller KD, Jemal A. Cancer statistics, 2018. CA Cancer J Clin. 2018 Jan;68(1):7-30.

4) Máire A. Duggan, William F. Anderson, Sean Altekruse, Lynne Penberthy, Mark E. Sherman. The surveillance, Epidemiology and End Results(SEER) Program and Pathology: Towards Strengthening the Critical Relationship. Am J Surg Pathol. Author manuscript; available in PMC 2017 Dec 1. Published in final edited form as: Am J Surg Pathol. 2016 Dec; 40(12): e94–e102.

5) Dean DC, Shen S, Hornicek FJ, Duan Z. From genomics to metabolomics: emerging metastatic biomarkers in osteosarcoma. Cancer Metastasis Rev. 2018 Dec;37(4):719-731.

6) Matthew D. Hellmann, Tavi Nathanson, Hira Rizvi, Benjamin C. Creelan, Francisco Sanchez-Vega, Arun Ahuja, Ai Ni, Jacki B. Novik, Levi M.B. Mangarin, Mohsen Abu-Akeel, Cailian Liu, Jennifer L. Sauter, Natasha Rekhtman, Eliza Chang, Margaret K. Callahan, Jamie E. Chaft, Martin H. Voss, Megan Tenet, Xue-Mei Li, Kelly Covello, Andrea Renninger, Patrik Vitazka, William J. Geese, Hossein Borghaei, Charles M. Rudin, Scott J. Antonia, Charles Swanton, Jeff Hammerbacher, Taha Merghoub, Nicholas McGranahan, Alexandra Snyder, Jedd D. Wolchok. Genomic Features of Response to Combination Immunotherapy in Patients with Advanced Non-Small-Cell Lung Cancer. Cancer Cell. 2018 May 14; 33(5): 843–852.

7) Hiro Sato, Atsuko Niimi, Takaaki Yasuhara, Tiara Bunga Mayang Permata, Yoshihiko Hagiwara, Mayu Isono, Endang Nuryadi, Ryota Sekine, Takahiro Oike, Sangeeta Kakoti, Yuya Yoshimoto, Kathryn D. Held, Yoshiyuki Suzuki, Koji Kono, Kiyoshi Miyagawa, Takashi Nakano, Atsushi Shibata. DNA double-strand break repair pathway regulates PD-L1 expression in cancer cells. Nat Commun. 2017; 8: 1751. Published online 2017 Nov 24. doi: 10.1038/s41467-017-01883-9.

8) Le Cesne A, Marec-Berard P, Blay JY, Gaspar N, Bertucci F, Penel N, Bompas E, Cousin S, Toulmonde M, Bessede A, Fridman WH, Sautes-Fridman C, Kind M, Le Loarer F, Pulido M, Italiano A. Programmed cell death 1 (PD-1) targeting in patients with advanced osteosarcomas: results from the PEMBROSARC study. Eur J Cancer. 2019 Sep;119:151-157.

9) Thanindratarn P, Dean DC, Nelson SD, Hornicek FJ, Duan Z. Advances in immune checkpoint inhibitors for bone sarcoma therapy. J Bone Oncol. 2019 Jan 29;15:100221.

10) Davoli T, Uno H, Wooten EC, Elledge SJ. Tumor aneuploidy correlates with markers of immune evasion and with reduced response to immunotherapy. Science (New York, NY). 2017. 355:6322.

11) Schiavone K, Garnier D, Heymann MF, Heymann D. The Heterogeneity of Osteosarcoma: The Role Played by Cancer Stem Cells. Adv Exp Med Biol. 2019;1139:187-200.

12) Wang D, Niu X, Wang Z, Song CL, Huang Z, Chen KN, Duan J, Bai H, Xu J, Zhao J, Wang Y, Zhuo M, Xie XS, Kang X, Tian Y, Cai L, Han JF, An T, Sun Y, Gao S, Zhao J, Ying J, Wang L, He J, Wang J. Multiregion Sequencing Reveals the Genetic Heterogeneity and Evolutionary History of Osteosarcoma and Matched Pulmonary Metastases. Cancer Res. 2019 Jan 1;79(1):7-20.

13) Schiavone K, Garnier D, Heymann MF, Heymann D. The Heterogeneity of Osteosarcoma: The Role Played by Cancer Stem Cells. Adv Exp Med Biol. 2019;1139:187-200.

14) Bousquet M, Noirot C, Accadbled F, Sales de Gauzy J, Castex MP, Brousset P, Gomez-Brouchet A. Whole-exome sequencing in osteosarcoma reveals important heterogeneity of genetic alterations. Ann Oncol. 2016 Apr;27(4):738-44.

15) Chen X, Bahrami A, Pappo A, Easton J, Dalton J, Hedlund E, Ellison D, Shurtleff S, Wu G, Wei L, et al. Recurrent somatic structural variations contribute to tumorigenesis in pediatric osteosarcoma. Cell Rep. 2014. 7(1):104–112.

16) Sun H, Liu L, Huang Q, Liu H, Huang M, Wang J, Wen H, Lin R, Qu K, Li K, Wei H, Xiao W, Sun R, Tian Z, Sun C. Accumulation of Tumor-Infiltrating CD49a+ NK Cells Correlates with Poor Prognosis for Human Hepatocellular Carcinoma. Cancer Immunol Res. 2019 Sep;7(9):1535-1546.

17) Josefsson SE, Beiske K, Blaker YN, Førsund MS, Holte H, Østenstad B, Kimby E, Köksal H, Wälchli S, Bai B, Smeland EB, Levy R, Kolstad A, Huse K, Myklebust JH. TIGIT and PD-1 Mark Intratumoral T Cells with Reduced Effector Function in B-cell Non-Hodgkin Lymphoma. Cancer Immunol Res. 2019 Mar;7(3):355-362.

18) Dixon KO, Schorer M, Nevin J, Etminan Y, Amoozgar Z, Kondo T, Kurtulus S, Kassam N, Sobel RA, Fukumura D, Jain RK, Anderson AC, Kuchroo VK, Joller N. Functional Anti-TIGIT Antibodies Regulate Development of Autoimmunity and Antitumor Immunity.J Immunol. 2018 Apr 15;200(8):3000-3007.

19) Andrews LP, Yano H, Vignali DAA. Inhibitory receptors and ligands beyond PD-1, PD-L1 and CTLA-4: breakthroughs or backups. Nat Immunol. 2019 Nov;20(11):1425-1434.

20) Atiye J, Wolf M, Kaur S, Monni O, Böhling T, Kivioja A, Tas E, Serra M, Tarkkanen M, Knuutila S.Gene amplifications in osteosarcoma-CGH microarray analysis. Genes Chromosomes Cancer. 2005 Feb;42(2):158-63.

21) Li H, Hong S, Qian J, Zheng Y, Yang J, Yi Q. Cross talk between the bone and immune systems: osteoclasts function as antigen-presenting cells and activate CD4+ and CD8+ T cells.

578 Blood. 2010 Jul 15;116(2):210-7.
579 22) Mun SH, Won HY, Hernandez P, Aguila HL, Lee SK. Deletion of CD74, a putative MIF
580 receptor, in mice enhances osteoclastogenesis and decreases bone mass. J Bone Miner
581 Res. 2013 Apr;28(4):948-59.
582 23) Hu G, Cheng Z, Wu Z, Wang H. Identification of potential key genes associated
583 with osteosarcoma based on integrated bioinformatics analyse. J Cell Biochem. 2019
584 Aug;120(8):13554-13561.
585 24) Peng J, Sun BF, Chen CY, Zhou JY, Chen YS, Chen H, Liu L, Huang D, Jiang J, Cui GS,
586 Yang Y, Wang W, Guo D, Dai M, Guo J, Zhang T, Liao Q, Liu Y, Zhao YL, Han DL, Zhao Y,
587 Yang YG, Wu W. Single-cell RNA-seq highlights intra-tumoral heterogeneity and malignant
588 progression in pancreatic ductal adenocarcinoma.Cell Res. 2019 Sep;29(9):725-738.
589 25) Torabi A, Amaya CN, Wians FH Jr, Bryan BA. PD-1 and PD-L1 expression in bone and soft
590 tissue sarcomas. Pathology. 2017 Aug;49(5):506-513.
591 26) Kansara M, Thomas DM. Molecular pathogenesis of osteosarcoma. DNA Cell Biol. 2007
592 Jan;26(1):1-18.
593 27) Han Y, Feng H, Sun J, Liang X, Wang Z, Xing W, Dai Q, Yang Y, Han A, Wei Z, Bi Q, Ji
594 H, Kang T, Zou W. Lkb1 deletion in periosteal mesenchymal progenitors induces osteogenic
595 tumors through mTORC1 activation. J Clin Invest. 2019 May 1;129(5):1895-1909.
596 28) Debnath S, Yallowitz AR, McCormick J, Lalani S, Zhang T, Xu R, Li N, Liu Y, Yang
597 YS, Eiseman M, Shim JH, Hameed M, Healey JH, Bostrom MP, Landau DA, Greenblatt MB.
598 Discovery of a periosteal stem cell mediating intramembranous bone formation. Nature. 2018
599 Oct;562(7725):133-139.
600 29) Chan CK, Seo EY, Chen JY, Lo D, McArdle A, Sinha R, Tevlin R, Seita
601 J, Vincent-Tompkins J, Wearda T, Lu WJ, Senarath-Yapa K, Chung MT, Marecic O, Tran
602 M, Yan KS, Upton R, Walmsley GG, Lee AS, Sahoo D, Kuo CJ, Weissman IL, Longaker
603 MT. Identification and specification of the mouse skeletal stem cell. Cell. 2015 Jan
604 15;160(1-2):285-98.
605 30) Suehara Y, Alex D, Bowman A, Middha S, Zehir A, Chakravarty D, Wang L, Jour G, Nafa K,
606 Hayashi T, Jungbluth AA, Frosina D, Slotkin E, Shukla N, Meyers P, Healey JH, Hameed M,
607 Ladanyi M. Clinical Genomic Sequencing of Pediatric and Adult Osteosarcoma Reveals
608 Distinct Molecular Subsets with Potentially Targetable Alterations. Clin Cancer Res. 2019
609 Nov 1;25(21):6346-635.
610 31) Osumi T, Miharu M, Fuchimoto Y, Morioka H, Kosaki K, Shimada H. The
611 germline TP53 mutation c.722 C>T promotes bone and liver tumorigenesis at a young age.
612 Pediatr Blood Cancer. 2012 Dec 15;59(7):1332-3.
613 32) Tang F, Min L, Seebacher NA, Li X, Zhou Y, Hornicek FJ, Wei Y, Tu C, Duan Z. Targeting
614 mutant TP53 as a potential therapeutic strategy for the treatment of osteosarcoma. J Orthop
615 Res. 2019 Mar;37(3):789-798.

33) Tawbi HA, Burgess M, Bolejack V, Van Tine BA, Schuetze SM, Hu J, D'Angelo S, Attia S, Riedel RF, Priebat DA, Movva S, Davis LE, Okuno SH, Reed DR, Crowley J, Butterfield LH, Salazar R, Rodriguez-Canales J, Lazar AJ, Wistuba II, Baker LH, Maki RG, Reinke D, Patel S. Pembrolizumab in advanced soft-tissue sarcoma and bone sarcoma (SARC028): a multicentre, two-cohort, single-arm, open-label, phase 2 trial.Lancet Oncol. 2017 Nov;18(11):1493-1501.

34) Paoluzzi L, Cacavio A, Ghesani M, Karambelkar A, Rapkiewicz A, Weber J, Rosen G. Response to anti-PD1 therapy with nivolumab in metastatic sarcomas. Clin Sarcoma Res. 2016 Dec 30;6:24.

35) Gomez-Brouchet A, Illac C, Gilhodes J, Bouvier C, Aubert S, Guinebretiere JM, Marie B, Larousserie F, Entz-Werlé N, de Pinieux G, Filleron T, Minard V, Minville V, Mascard E, Gouin F, Jimenez M, Ledeley MC, Piperno-Neumann S, Brugieres L, Rédini F. CD163-positive tumor-associated macrophages and CD8-positive cytotoxic lymphocytes are powerful diagnostic markers for the therapeutic stratification of osteosarcoma patients: An immunohistochemical analysis of the biopsies fromthe French OS2006 phase 3 trial. Oncoimmunology. 2017 Aug 24;6(9):e1331193.

36) Alves PM, de Arruda JAA, Arantes DAC, Costa SFS, Souza LL, Pontes HAR, Fonseca FP, Mesquita RA, Nonaka CFW, Mendonça EF, Batista AC. Evaluation of tumor-infiltrating lymphocytes in osteosarcomas of the jaws: a multicenter study. Virchows Arch. 2019 Feb;474(2):201-207

37) Palmerini E, Agostinelli C, Picci P, Pileri S, Marafioti T, Lollini PL, Scotlandi K, Longhi A, Benassi MS, Ferrari S. Tumoral immune-infiltrate (IF), PD-L1 expression and role of CD8/TIA-1 lymphocytes in localized osteosarcoma patients treated within protocol ISG-OS1. Oncotarget. 2017 Dec 4;8(67):111836-111846.

38) Koirala P, Roth ME, Gill J, Piperdi S, Chinai JM, Geller DS, Hoang BH, Park A, Fremed MA, Zang X, Gorlick R. Immune infiltration and PD-L1 expression in the tumor microenvironment are prognostic in osteosarcoma. Sci Rep. 2016 Jul 26;6:30093.

39) Zheng W, Xiao H, Liu H, Zhou Y. Expression of programmed death 1 is correlated with progression of osteosarcoma. APMIS. 2015 Feb;123(2):102-7.

40) Wang D, Niu X, Wang Z, Song CL, Huang Z, Chen KN, Duan J, Bai H, Xu J, Zhao J, Wang Y, Zhuo M, Xie XS, Kang X, Tian Y, Cai L, Han JF, An T, Sun Y, Gao S, Zhao J, Ying J, Wang L, He J, Wang J. Multiregion Sequencing Reveals the Genetic Heterogeneity and Evolutionary History of Osteosarcoma and Matched Pulmonary Metastases. Cancer Res. 2019 Jan 1;79(1):7-20.

41) Stamm H, Oliveira-Ferrer L, Grossjohann EM, Muschhammer J, Thaden V, Brauneck F, Kischel R, Müller V, Bokemeyer C, Fiedler W, Wellbrock J. Targeting the TIGIT-PVR immune checkpoint axis as novel therapeutic option in breast cancer. Oncoimmunology. 2019 Oct 12;8(12):e1674605.

42) Hoogi S, Eisenberg V, Mayer S, Shamul A, Barliya T, Cohen CJ. A TIGIT-based chimeric co-stimulatory switch receptor improves T-cell anti-tumor function. J Immunother Cancer. 2019 Sep 9;7(1):243.

43) Washburn ML, Wang Z, Walton AH, Goedegebuure SP, Figueroa DJ, Van Horn S, Grossman J, Remlinger K, Madsen H, Brown J, Srinivasan R, Wolf AI, Berger SB, Yi VN, Hawkins WG, Fields RC, Hotchkiss RS. T Cell- and Monocyte-Specific RNA-Sequencing Analysis in Septic and Nonseptic Critically Ill Patients and in Patients with Cancer. J Immunol. 2019 Oct 1;203(7):1897-1908.

44) Zhang Q, Bi J, Zheng X, Chen Y, Wang H, Wu W, Wang Z, Wu Q, Peng H, Wei H, Sun R, Tian Z. Blockade of the checkpoint receptor TIGIT prevents NK cell exhaustion and elicits potent anti-tumor immunity. Nat Immunol. 2018 Jul;19(7):723-732.

45) Dumars C, Ngyuen JM, Gaultier A, Lanel R, Corradini N, Gouin F, Heymann D, Heymann MF. Dysregulation of macrophage polarization is associated with the metastatic process in osteosarcoma. Oncotarget. 2016 Nov 29;7(48):78343-78354.

46) Brard C, Piperno-Neumann S, Delaye J, Brugières L, Hampson LV, Le Teuff G, Le Deley MC, Gaspar N. Sarcome-13/OS2016 trial protocol: a multicentre, randomised, open-label, phase II trial of mifamurtide combined with postoperative chemotherapy for patients with newly diagnosed high-risk osteosarcoma. BMJ Open. 2019 May 19;9(5):e02587.

47) Su S, Chen J, Yao H, Liu J, Yu S, Lao L, Wang M, Luo M, Xing Y, Chen F, Huang D, Zhao J, Yang L, Liao D, Su F, Li M, Liu Q, Song E. CD10+GPR77+ Cancer-Associated Fibroblasts Promote Cancer Formation and Chemoresistance by Sustaining Cancer Stemness..Cell. 2018 Feb 8;172(4):841-856.e16.

48) Fearon DT. The carcinoma-associated fibroblast expressing fibroblast activation protein and escape from immune surveillance. Cancer Immunol Res. 2014 Mar;2(3):187-93.

49) Elyada E, Bolisetty M, Laise P, Flynn WF, Courtois ET, Burkhart RA, Teinor JA, Belleau P, Biffi G, Lucito MS, Sivajothi S, Armstrong TD, Engle DD, Yu KH, Hao Y, Wolfgang CL, Park Y, Preall J, Jaffee EM, Califano A, Robson P, Tuveson DA. Cross-Species Single-Cell Analysis of Pancreatic Ductal Adenocarcinoma Reveals Antigen-Presenting Cancer-Associated Fibroblasts. Cancer Discov. 2019 Aug;9(8):1102-1123.

50) An Y, Liu F, Chen Y, Yang Q. Crosstalk between cancer-associated fibroblasts and immune cells in cancer. J Cell Mol Med. 2019 Oct 23. doi: 10.1111/jcmm.14745.

Tables and Figure Legends

Table 1. Clinical Characteristics of OS Patients

Fig. 1 Delineation of diverse cell types in OS using the scRNA-seq method.

(A) The t-SNE plot displayed the main cell types in OS tissue. (B) Violin plots demonstrated the expression levels of cluster-specific marker genes. (C) Dot plot displayed multiple well-known cell type-specific biomarkers across clusters. The size of dots represents the proportion of cells expressing a particular marker, and the spectrum of color indicates the mean level of this gene. Legends are shown as above. (D) Heatmap showed the significant gene in each cell group.

Fig. 2. Differential gene expression profiles in malignant OS cells.

(A) The malignant osteoblast cells, here named OS, were divided into 5 subtypes based on t-SNE analysis. (B) The characteristics of 5 subgroups. OS cells were differentiated by GO analysis. (C) The trajectory analysis of the OS cells included primary, metastasis and recurrence. (D) The primary OS cells gathered 4 clusters. For primary and metastatic OS cells, the differentially expressed genes (rows) in conformity with the pseudo-time (columns) gathered hierarchically into 6 cluster profiles. For primary and recurrent OS gene profiles, 6 clusters were gathered. Furthermore, we outlined the corresponding diagram on the basis of the transcription factor data. Color key from blue to red indicates relative expression levels from low to

high.

Fig. 3. Distinct subpopulations of osteoclastic cells based on scRNA-seq data.

(A) Graphical (t-SNE) plot demonstrated 3 main cell subtypes of OC. (B)We also showed the t-SNE plot figure marked ACP5, CTSK, CD74 and TOP2A separately. (C) Pseudo-time figure showed the development of OC subpopulations. We also presented the Pseudo-time marked ACP5, CTSK, CD74 and TOP2A respectively. (D) Different cell subtype clusters are color coded. The OC subtypes were classified according to the expression levels of specific genes represented in the heatmap. The GO analysis displayed the significant differences among 3 clusters. (E) The row graph was gathered hierarchically into 5 clusters. (F) We detected the expression of CD74 and CTSK in OS samples by IHC.

Fig. 4. Identificaion of CAF subtypes in OS tissue.

(A) Unsupervised clustering of two CAF cells from OS samples represented in a t-SNE plot graph. Different cell type clusters were color coded. (B) Violin plots of selected apCAF and mCAF markers, showing normalized expression in two of the subclusters. (C) Many specific genes were uniquely upregulated in the apCAF subtype, including HLA-DRA, CD74, APOE *etc*.

Fig. 5. Single-cell analysis of myloid cells in OS samples.

(A) t-SNE plot of the myeloid cell subgroup in OS tumor samples. (B) M2-polorized markers CD163 and MRC1/CD206 were expressed in almost all TAMs. (C) The relative expression levels of the well-known biomarkers of each cell type as indicated in the violin plots. (D) Bubble plot was used to identify each cell type–specific markers across clusters. Size of dots represents fraction of cells expressing a particular marker, and intensity of color indicates level of mean expression.

Fig. 6. Subgroups of TILs in the OS tumor.

(A）Reclustering of the subgroup of TILs in the OS data represented in the t-SNE plot. Proportion of each subgroup cells in primary, recurrent and pulmonary metastatic tumor samples was provided. The tab exhibited the concrete value of each scRNA-seq sample gained. (B) Microscopy of the expression of CD3, CD4 and CD8 in primary,

recurrent and pulmonary metastatic OS tissues. Black scale bar is 100 μm. (C) The violin plots expound normalized levels of markers in the different subclusters. (D) The well-known markers of each cell population were represented in dot plot.

Fig. 7. Blockade of the TIGIT increases the specific lysis of breast cancer cell lines.

(A) Immunostaining of TIGIT in 11 OS tissue displayed dark brown. Scale bar: 100 μm. (B) We analyzed the lysis of the cytokine-induced killer cells (CIKs) produced from OS patients(n = 2) with or without blocking TIGIT on the OS cell line U2OS and 143B. Results of cytotoxicity ratio are depicted as the mean ± SD. For statistical analysis paired T-tests were performed (* means $p < 0.05$)

Fig. S1. The t-SNE analysis of individual

(A) The t-SNE results of 11 samples were shown on the list. The cell number and percentage of assigned cell types were summarized in the right panel. Cell number of all clusters were summarized in the right tab. (B) The t-SNE were gathered by region.

Fig. S2. The analysis of key genes in OS cells

(A) The KEGG analysis of OS cells was shown on the list. (B) The remarkable genes of each subtype were enriched in heatmep.

Fig. S3. The CNV analysis of OS cells

(A) The CNV analysis of primary OS cells revealed amplication of the chromosome 21 and 7 in almost all samples. (B) The CNV analysis of lung metastatic OS cells showed rare del in all chromosomes. (C) The CNV analysis of recurrent OS cells also exhibited amplication of the chromosome 21,7.

Fig. S4. The t-SNE analysis of TILs from OS different location

(A) The t-SNE results of TILs from primary OS tissue. (B) The t-SNE results of TILs from lung metastasis OS tissue. (C) The t-SNE results of TILs from recurrent OS tissue.

Fig. S5. The co-expression of CD74 and CTSK in OCs at different OS tissue

(A) The OC cells with CD74 and CTSK expression in primary OS tissue. (B) The OC

790 cells with CD74 and CTSK expression in recurrent OS tissue. (C) The OC cells with
791 CD74 and CTSK expression in lung metastasis OS tissue.(The CD74 positive cell
792 presented red color, the CTSK positive cell presented green color, the nuclear was
793 stain blue color)

794

795 **Table 1. Clinical Characteristics of OS Patients**

Sample	Gender	Age	pathological type	Type	location	Preoperative chemotherapy	Size(cm)	Necrosis rate	Ki67
BC2	male	11	conventional	Insitu	Femur	4 times(MTX,AP,IFO,MTX)	5.5*5*3	<90%	50%
BC3	Female	11	conventional	Insitu	Tibia	6 times(MTX,AP,MTX,AP, MTX,MTX)	8*6*6	<90%	70%
BC5	Female	19	conventional	Insitu	Fibula	3 times(MTX,IFO,AP)	8*7.5*6	≥90%	80%
BC6	Female	23	conventional	Insitu	Ulna	3 times(MTX,IFO,AP)	7*7*4	≥90%	15%
BC10	Female	19	conventional	Metastasis (Lung)	Femur	2 times(GT)	3.5*3*2	<90%	8%
BC11	male	12	conventional	Recurrent	Femur	3 times(GT)	20*11*10	<90%	30%
BC16	male	11	conventional	Insitu	Tibia	4 times(IFO,ADM+Lobapltin,MTX,MTX)	6*4*2.5	<90%	40%
BC17	Female	32	chondroblast	Metastasis (Lung)	Tibia	3 times(GT)	2*2*1.5	<90%	40%
BC20	male	9	Chondroblast	Recurrent	Femur	4 times(ADM+VP-16+ ADM+VP-16)	10*8*5	<90%	50%
BC21	Female	38	intraosseous osteosarcoma	Insitu	Femur	4 times(MTX,AP,IFO,AP)	5*4*1	<90%	10%
BC22	male	15	chondroblast	Insitu	Femur	4 times (MTX,AP,IFO,MTX)	18*15*12	<90%	20%

796

797

Figure 1

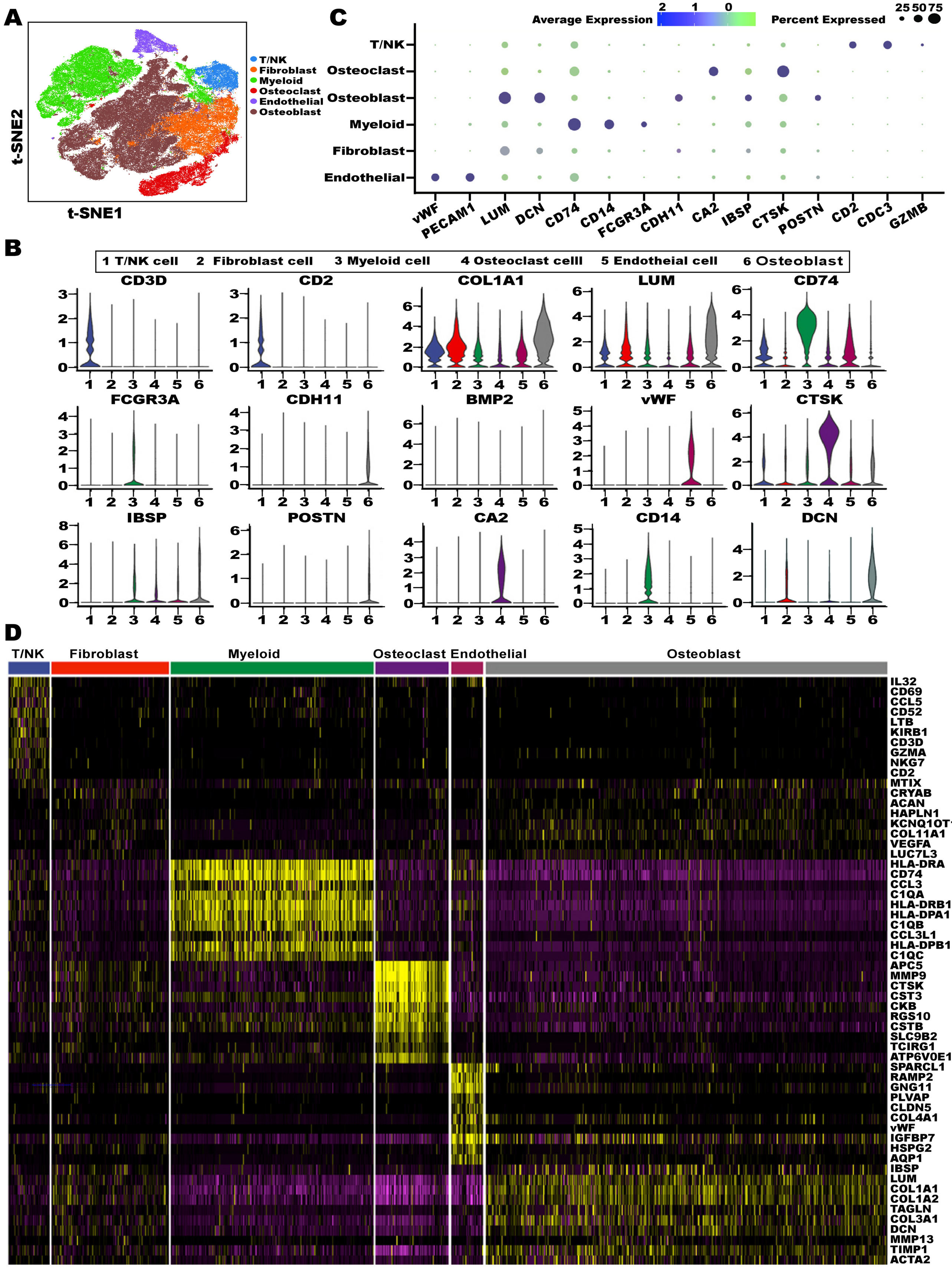
A
t-SNE2
t-SNE1
T/NK
Fibroblast
Myeloid
Osteoclast
Endothelial
Osteoblast
C
Average Expression
2
1
0
Percent Expressed
25
50
75
T/NK
Osteoclast
Osteoblast
Myeloid
Fibroblast
Endothelial
vWF
PECAM1
LUM
DCN
CD74
CD14
FCGR3A
CDH11
CA2
IBSP
CTSK
POSTN
CD2
CDC3
GZMB
B
1 T/NK cell
2 Fibroblast cell
3 Myeloid cell
4 Osteoclast celll
5 Endotheial cell
6 Osteoblast
CD3D
CD2
COL1A1
LUM
CD74
FCGR3A
CDH11
BMP2
vWF
CTSK
IBSP
POSTN
CA2
CD14
DCN
D
T/NK
Fibroblast
Myeloid
Osteoclast
Endothelial
Osteoblast
IL32
CD69
CCL5
CD52
LTB
KIRB1
CD3D
GZMA
NKG7
CD2
MTIX
CRYAB
ACAN
HAPLN1
KCNQ1OT1
COL11A1
VEGFA
LUC7L3
HLA-DRA
CD74
CCL3
C1QA
HLA-DRB1
HLA-DPA1
C1QB
CCL3L1
HLA-DPB1
C1QC
APC5
MMP9
CTSK
CST3
CKB
RGS10
CSTB
SLC9B2
TCIRG1
ATP6V0E1
SPARCL1
RAMP2
GNG11
PLVAP
CLDN5
COL4A1
vWF
IGFBP7
HSPG2
AQP1
IBSP
LUM
COL1A1
COL1A2
TAGLN
COL3A1
DCN
MMP13
TIMP1
ACTA2

Figure 2

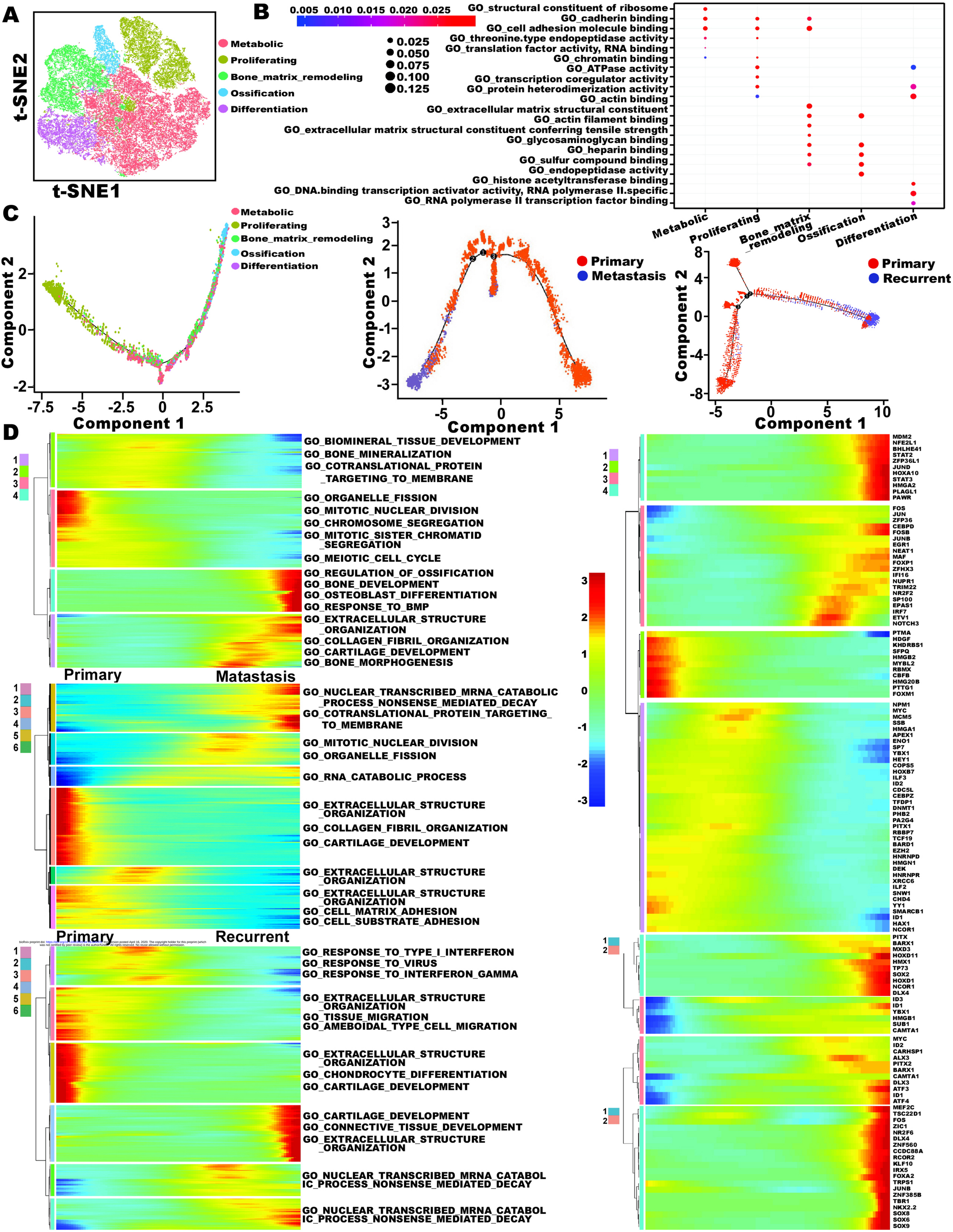

Figure 3

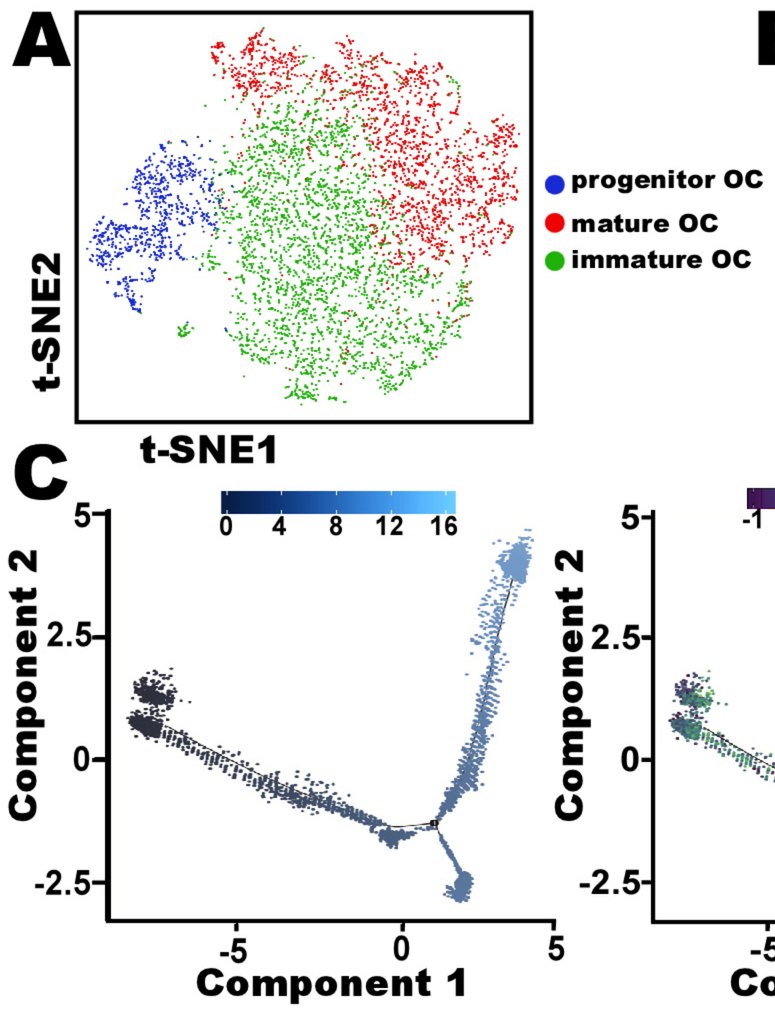

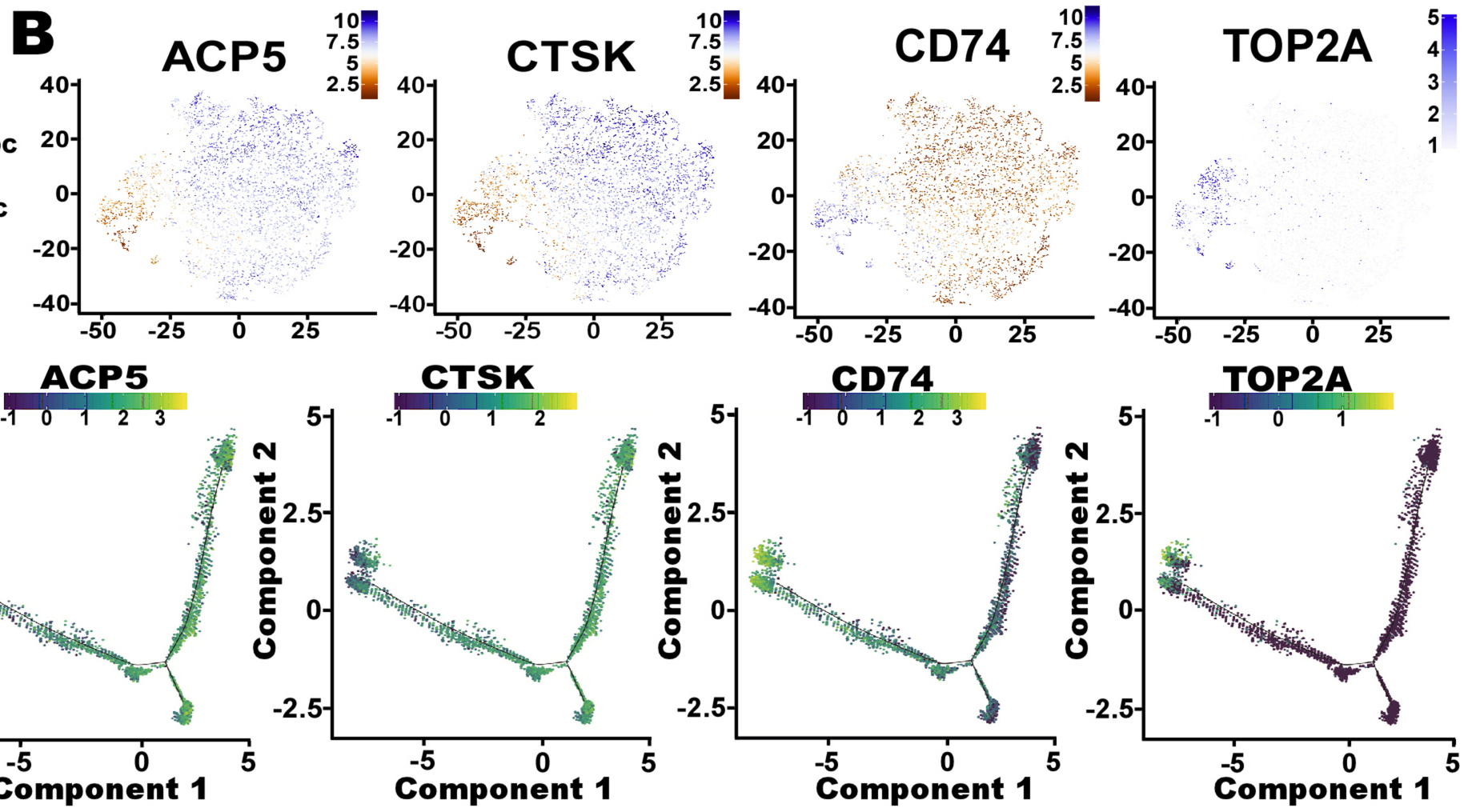

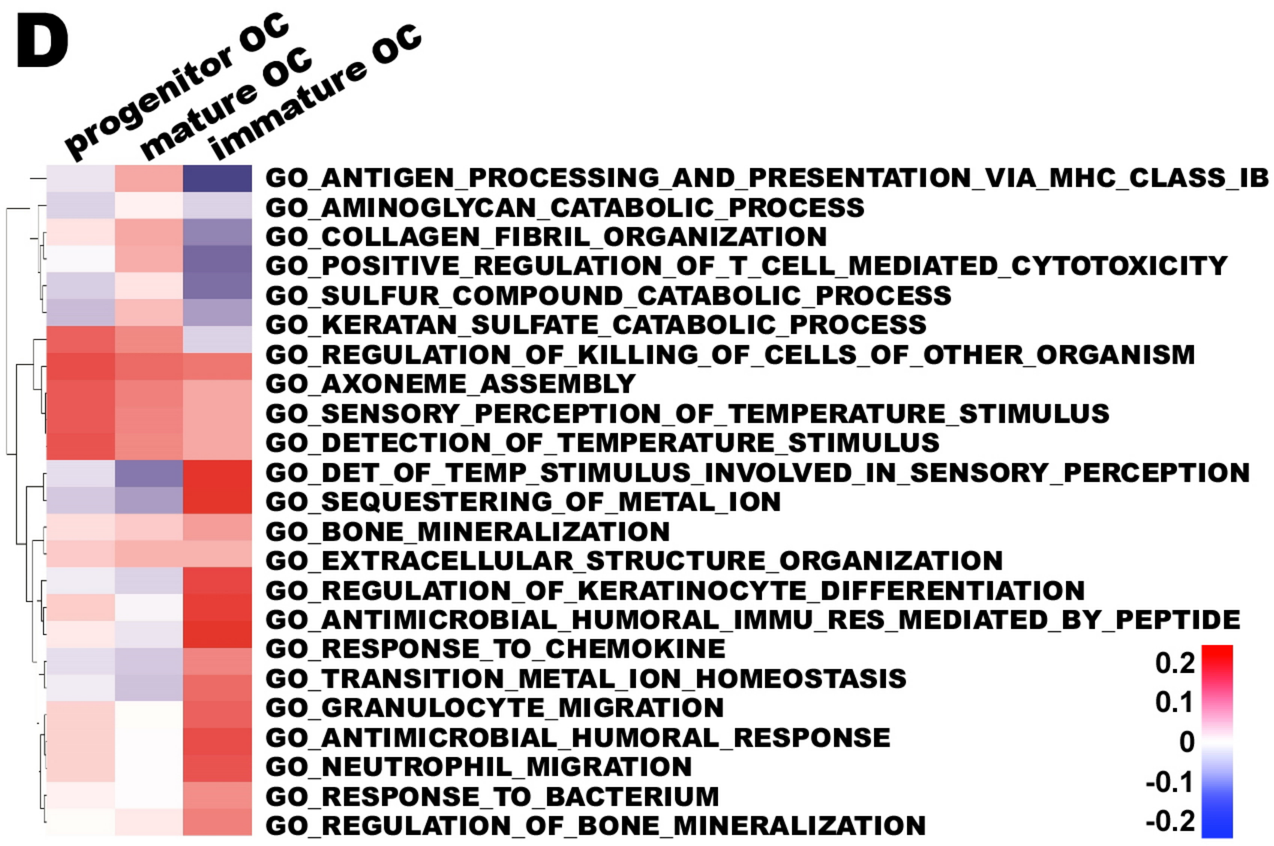

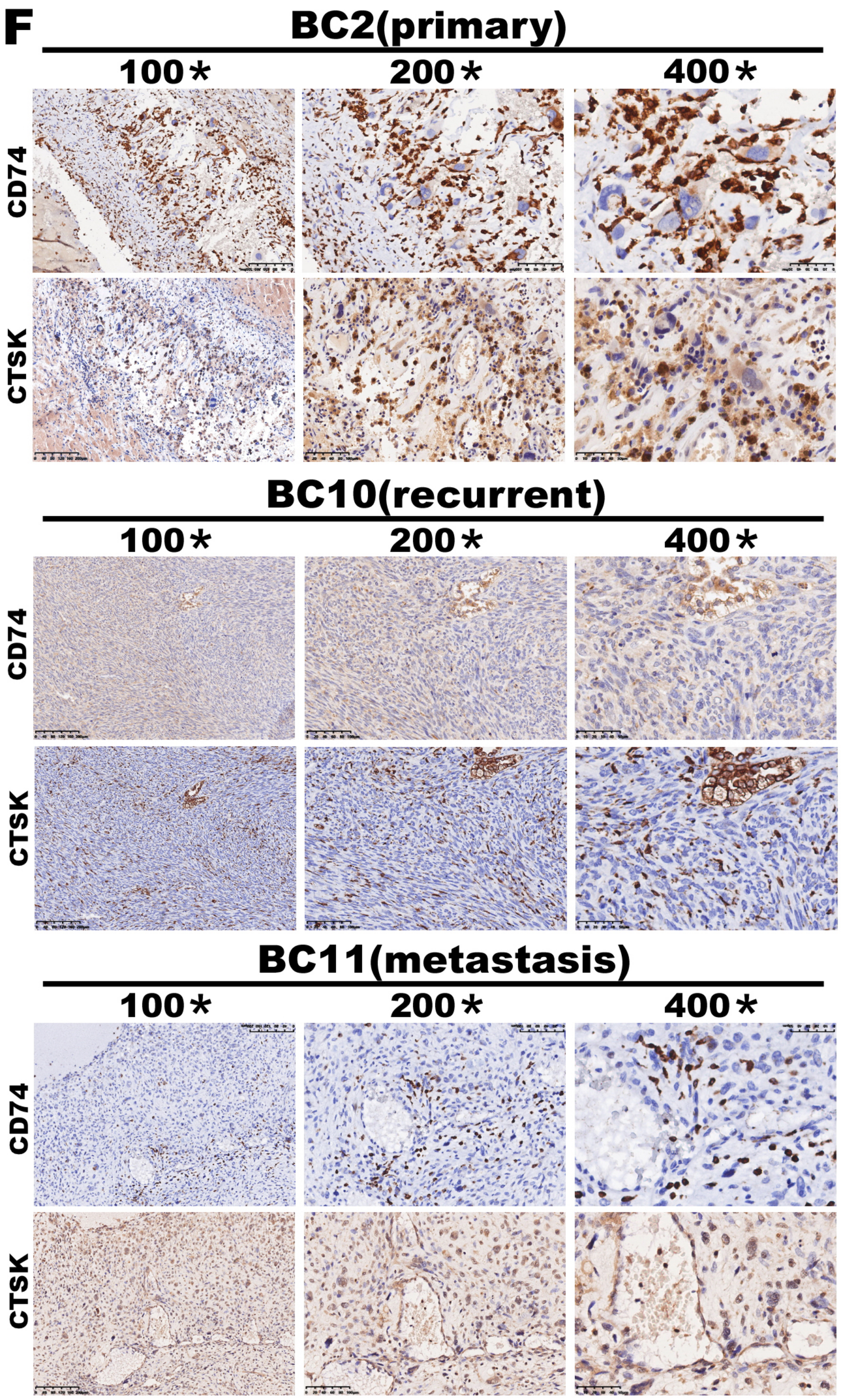

FIgure 4

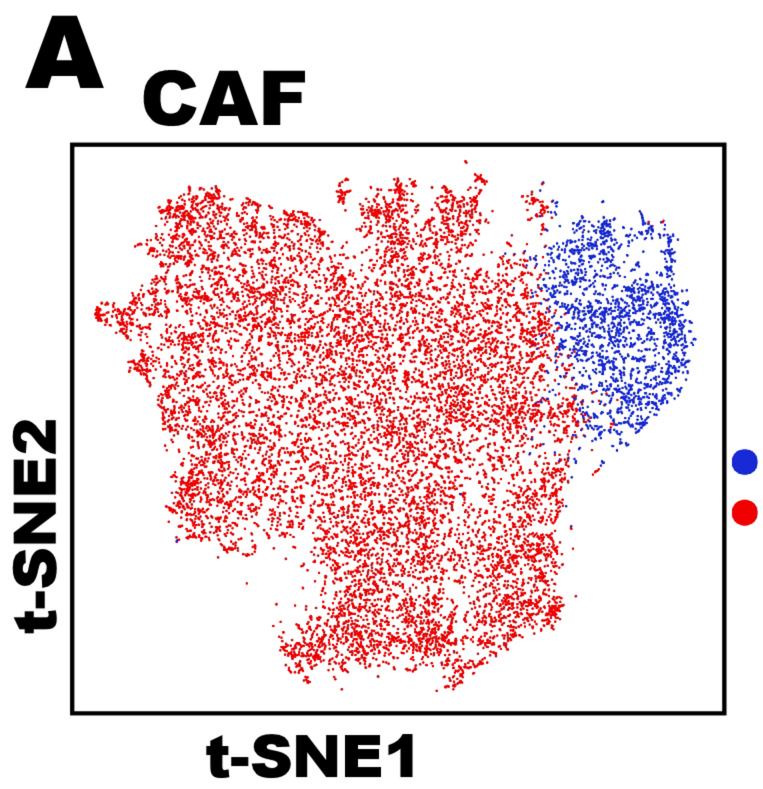

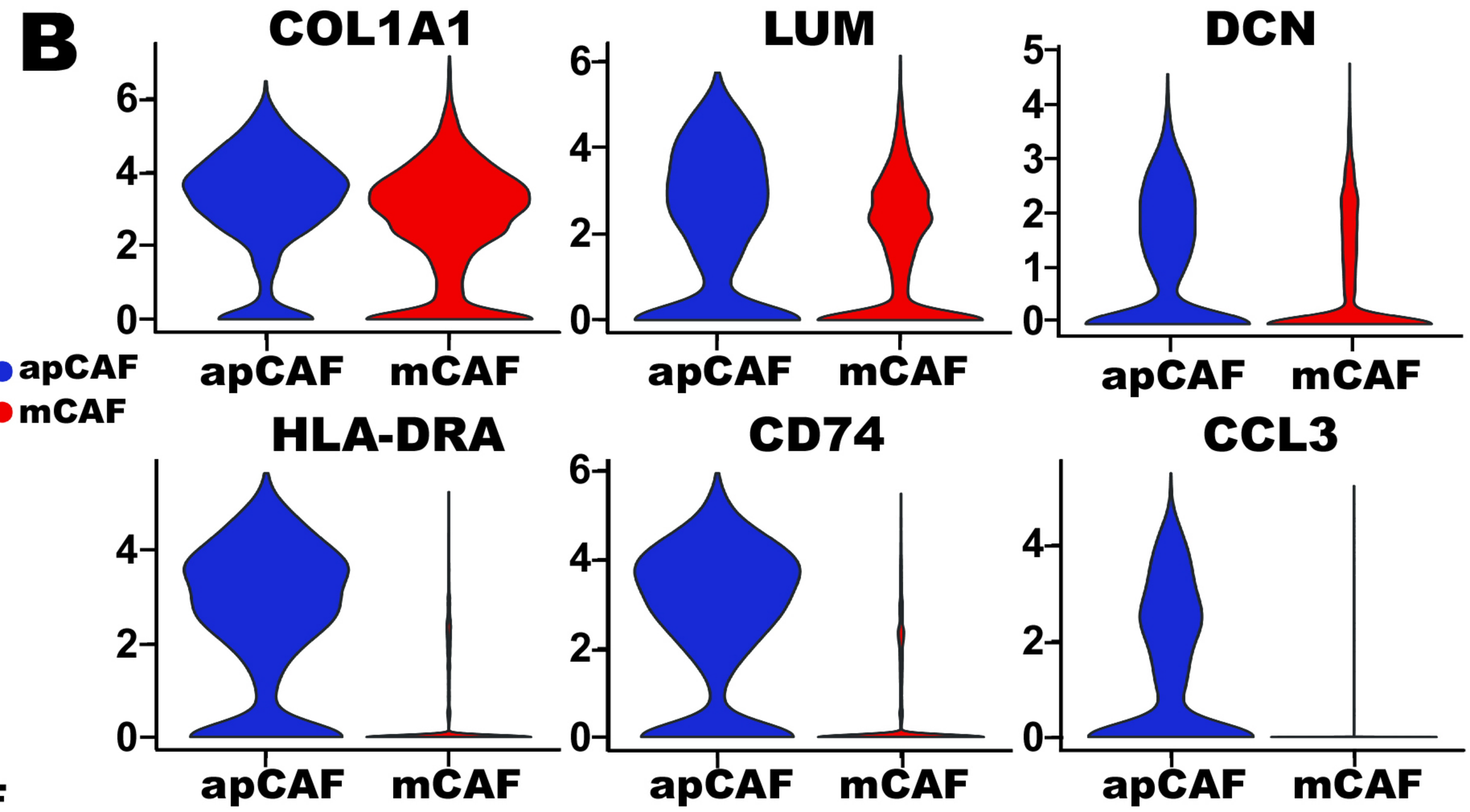

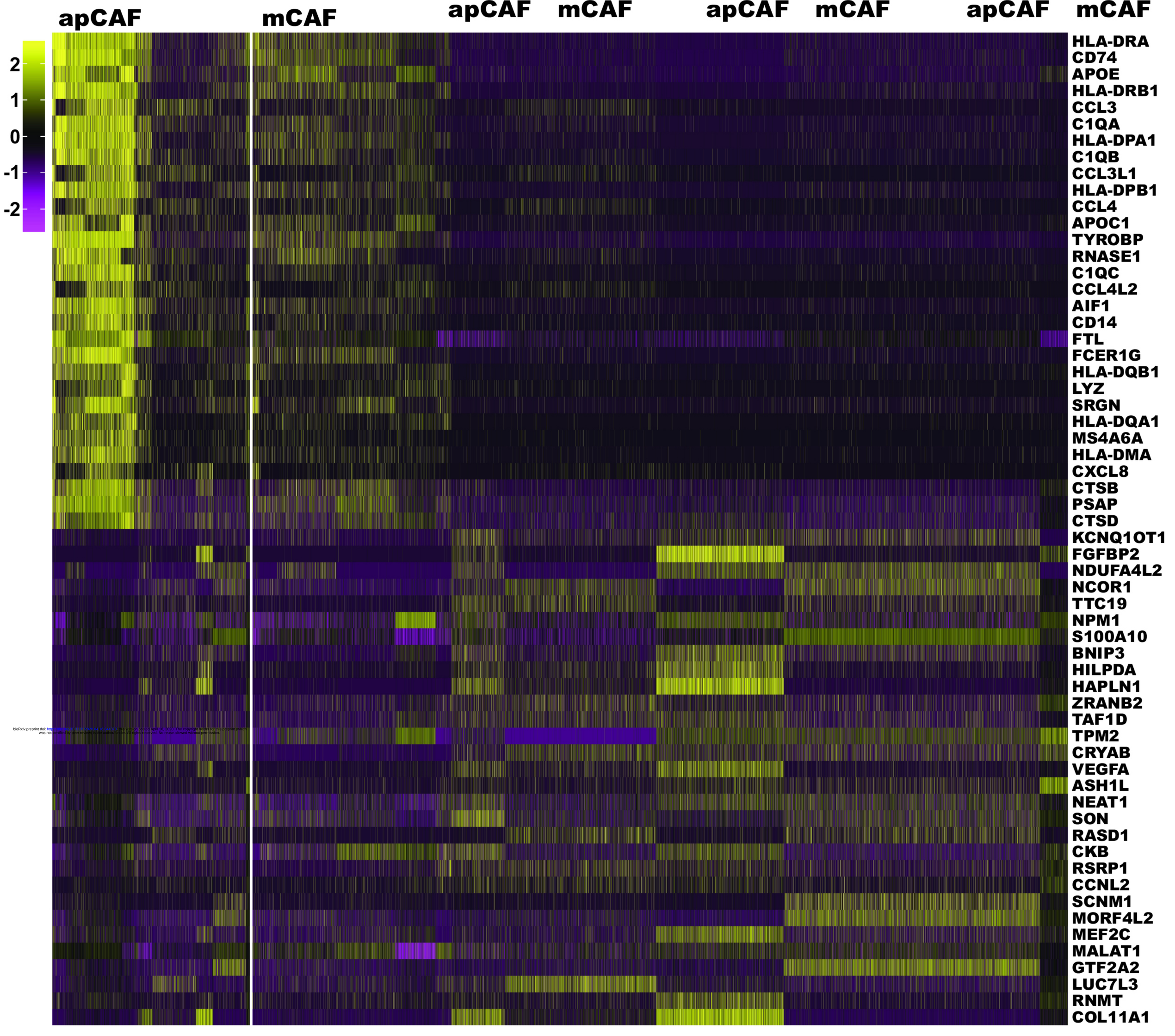

Figure 5

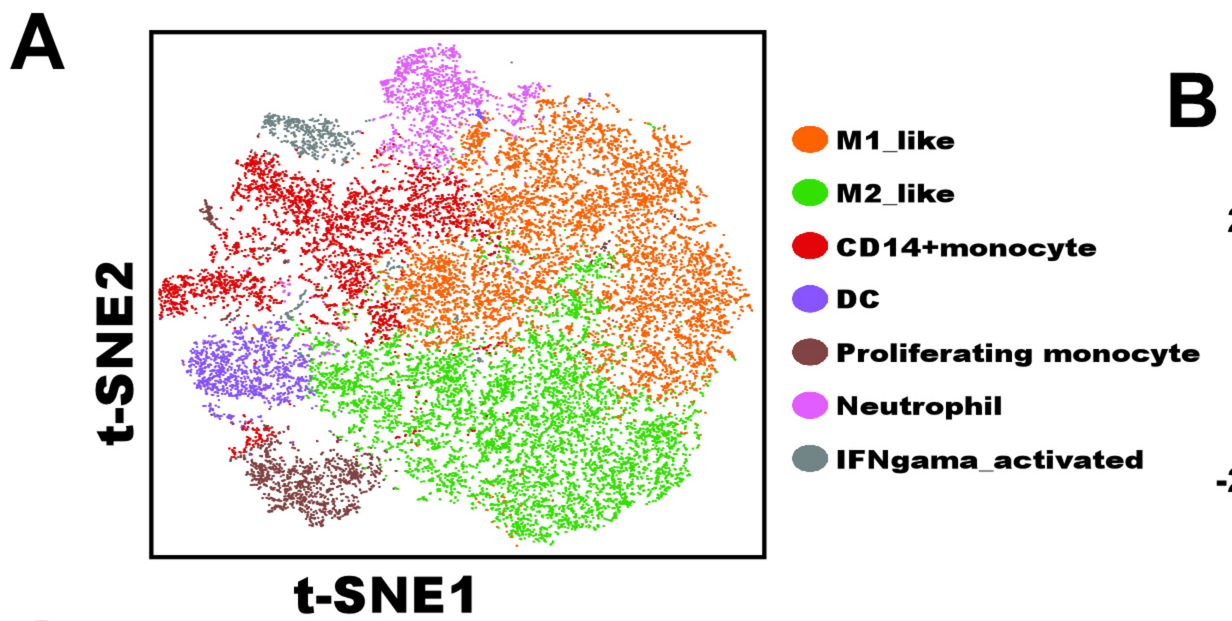

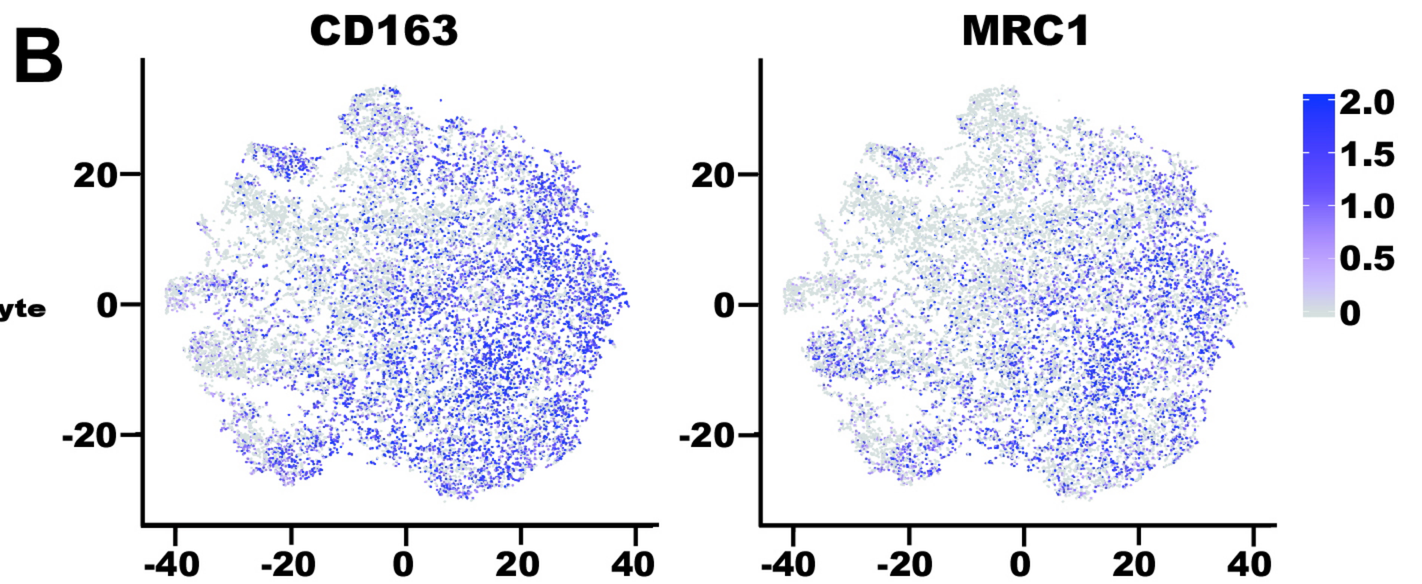

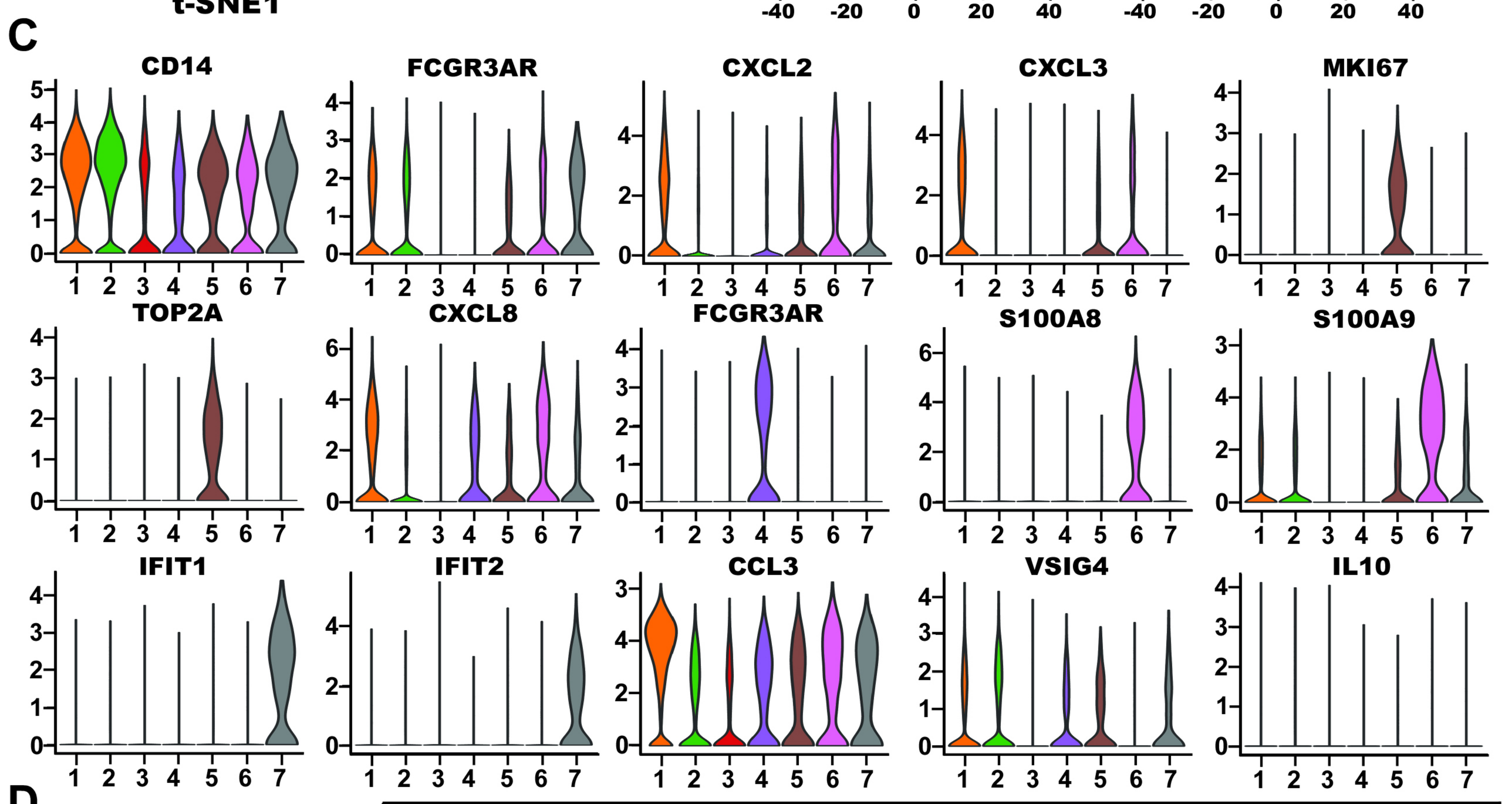

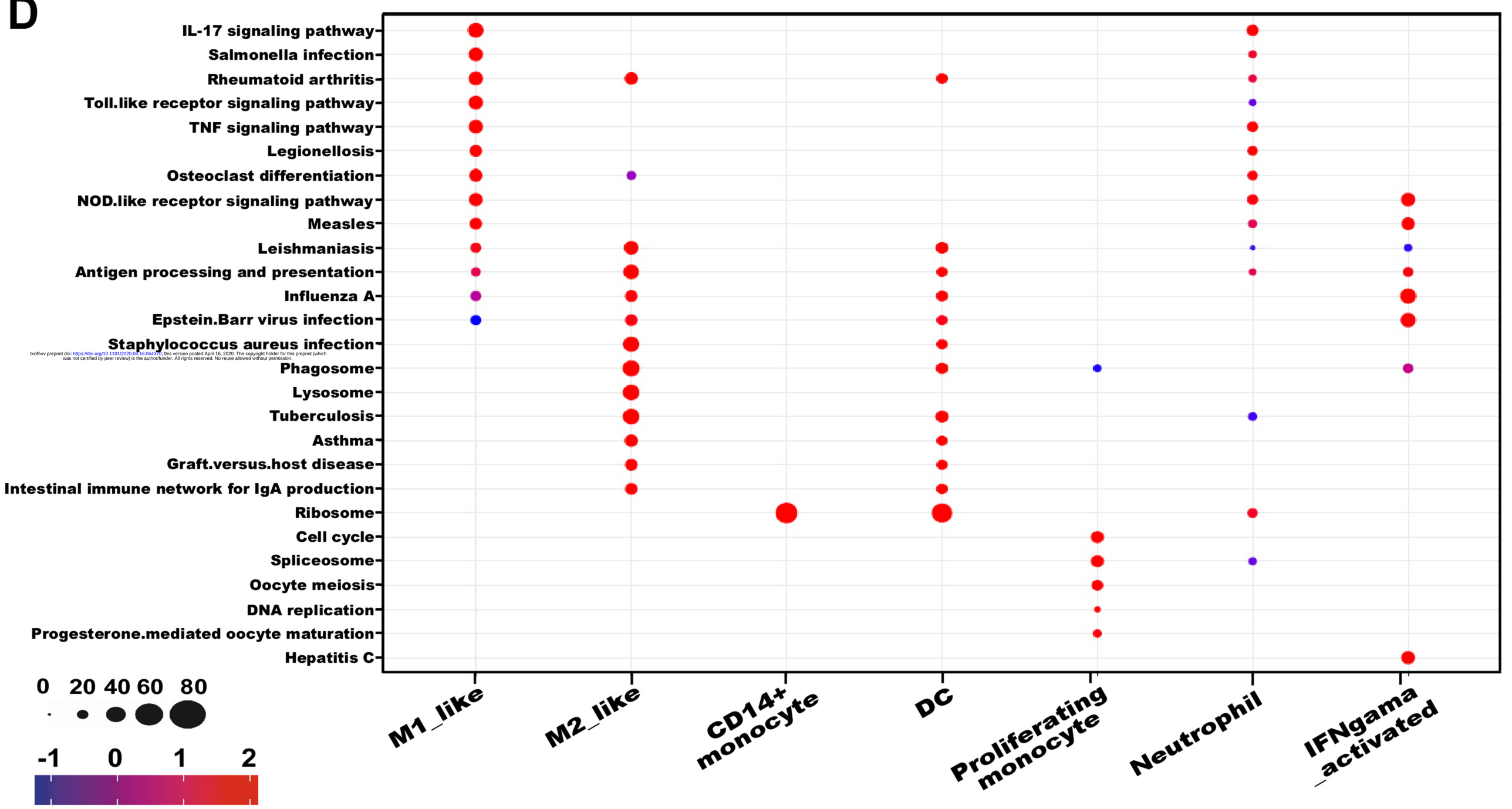

Figure 6

A

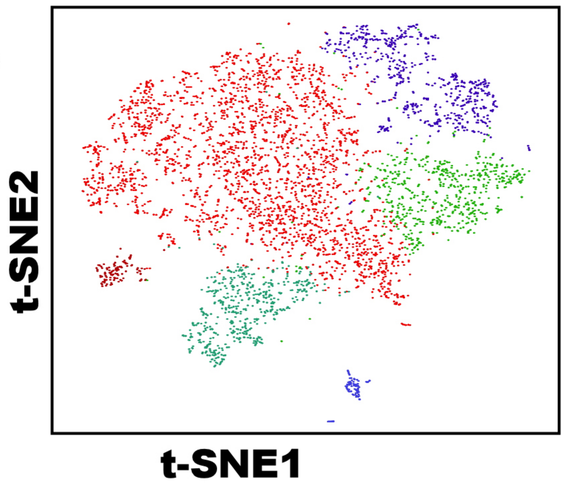

Cell type	In situ	Lung metatstasis	Recurrence	Total
CD4-/CD8- T cell	1148	1481	117	2746
CD8+ T cell	452	177	22	651
NK cell	464	126	50	640
T-reg cell	194	311	37	542
Plasma cell	114	2	1	117
Mast cell	94	4	1	99

B

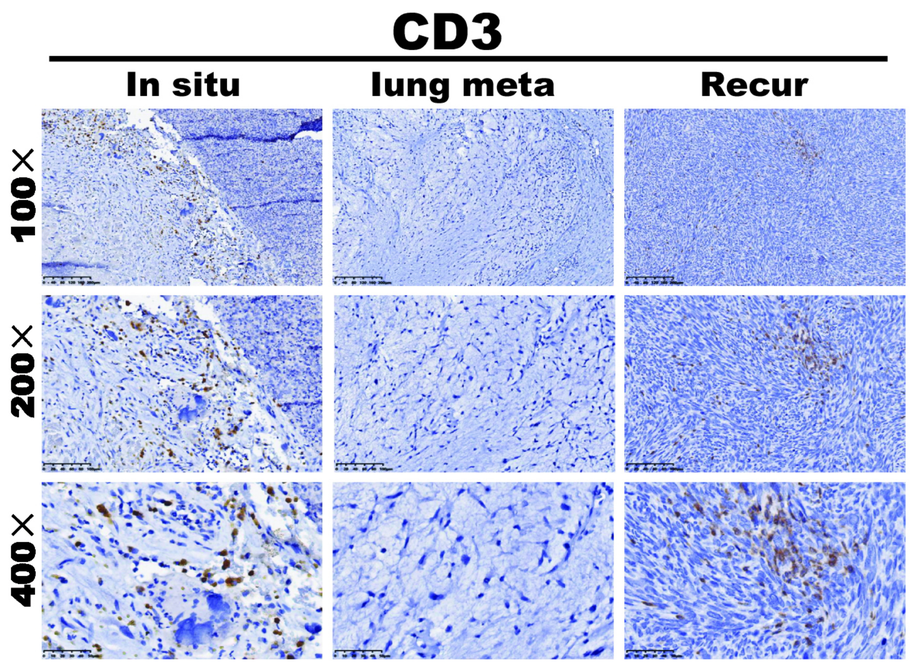

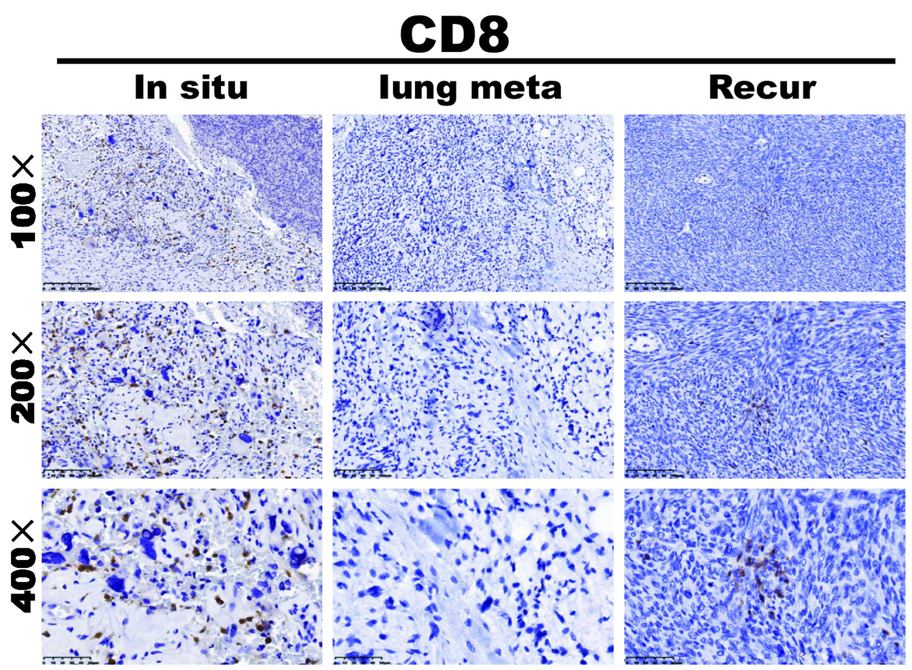

C

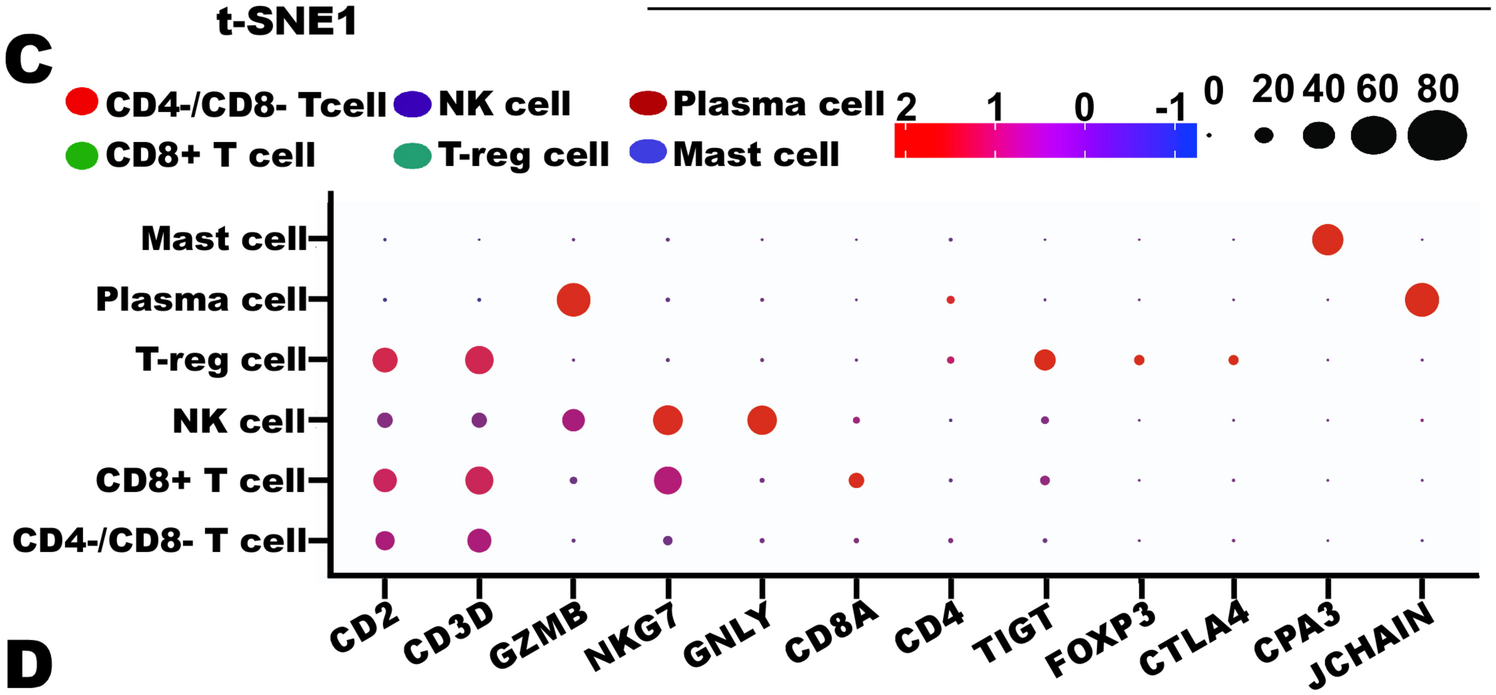

D

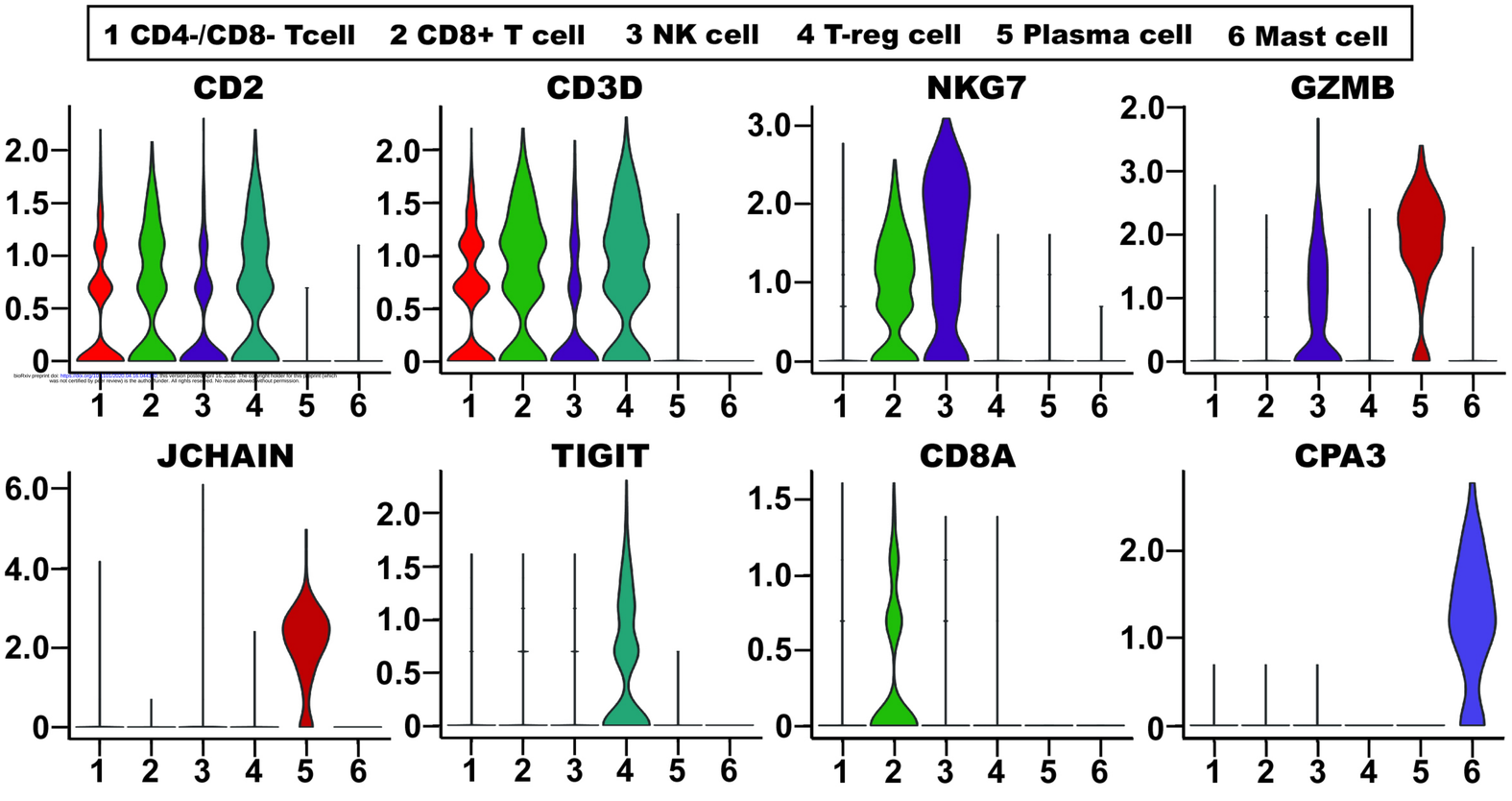

Figure 7